Theory of stellar convection – II. First stellar models

S. Pasetto,[1]★ C. Chiosi,[2] E. Chiosi,[3] M. Cropper[1] and A. Weiss[4]

[1]*University College London, Department of Space and Climate Physics, Mullard Space Science Laboratory, Holmbury St. Mary Dorking, Surrey RH5 6NT, UK*
[2]*Department of Physics and Astronomy, 'Galileo Galilei', University of Padua, Vicolo dell'Osservatorio 2, I-35122 Padova, Italy*
[3]*INAF–Osservatorio Astronomico di Padova, Vicolo dell'Osservatorio 5, I-35122 Padua, Italy*
[4]*Max-Planck-Institut für Astrophysik, Karl-Schwarzschild-Str. 1, D-85748 Garching bei München, Germany*

ABSTRACT

We present here the first stellar models on the Hertzsprung–Russell diagram, in which convection is treated according to the new scale-free convection theory (SFC theory) by Pasetto et al. The aim is to compare the results of the new theory with those from the classical, calibrated mixing-length (ML) theory to examine differences and similarities. We integrate the equations describing the structure of the atmosphere from the stellar surface down to a few per cent of the stellar mass using both ML theory and SFC theory. The key temperature over pressure gradients, the energy fluxes, and the extension of the convective zones are compared in both theories. The analysis is first made for the Sun and then extended to other stars of different mass and evolutionary stage. The results are adequate: the SFC theory yields convective zones, temperature gradients ∇ and ∇_e, and energy fluxes that are very similar to those derived from the 'calibrated' MT theory for main-sequence stars. We conclude that the old scale dependent ML theory can now be replaced with a self-consistent scale-free theory able to predict correct results, as it is more physically grounded than the ML theory. Fundamentally, the SFC theory offers a deeper insight of the underlying physics than numerical simulations.

Key words: convection – Sun: evolution – Hertzsprung–Russell and colour – magnitude diagrams – stars: horizontal branch.

1 INTRODUCTION

Convection is one of the fundamental mechanisms for carrying energy throughout a star from the deep interior to the outermost layers. This may happen during the pre-main-sequence, Hayashi phase of stars of any mass that are fully convective, during the main-sequence phase in central cores of stars more massive than about 1.3 M$_\odot$, in the main-sequence phase of very low mass stars (lower that about 0.3 M$_\odot$) that remain fully convective, and in the central cores of all stars burning helium (and in massive stars) heavier fuels up to iron. Convection occurs also in intermediate convective shells of some stars, in the outermost layers of stars of any mass where ionization of light elements occurs, and in very deep convective envelopes of red giant branch (RGB) and asymptotic giant branch (AGB) stars. Convection is present in white dwarfs, in the internal regions of stars in pre-supernova stages, during the collapse phase of Type II SNae, and the carbon-deflagration stages of Type Ia SNae. Convection is therefore ubiquitous in stars of any mass and evolutionary phase: it contributes significantly in the transport of energy across the layers of a star, from the deep interior to the surface and substantially changes the structure of a star by mixing the material across it.

In a star, convection sets in where and when the condition $\nabla_{rad} < \nabla_{ad}$ is violated, where ∇_{rad} and ∇_{ad} are the radiative and adiabatic logarithmic temperature gradient with respect to pressure, i.e. $\nabla_{rad} \equiv \left| \frac{d \ln T}{d \ln P} \right|_{rad}$ and $\nabla_{ad} \equiv \left| \frac{d \ln T}{d \ln P} \right|_{ad}$ (e.g. Cox & Giuli 1968; Kippenhahn, Weigert & Weiss 2012). While in the inner convective regions of a star the large thermal capacity of convective elements induces a temperature over pressure gradient of the medium, $\nabla \equiv \left| \frac{d \ln T}{d \ln P} \right|$, that is nearly adiabatic, i.e. $\nabla - \nabla_{ad} \simeq 10^{-8} \simeq 0$, in the outer layers both the temperature gradients of the medium and of the element $\nabla_e \equiv \left| \frac{d \ln T}{d \ln P} \right|_e$ differ significantly from ∇_{ad} (superadiabaticity). Convective elements in these regions have low thermal capacity and thus the approximation $\nabla - \nabla_{ad} \simeq 0$ can no longer be applied: ∇_e and ∇ must be determined separately to determine the amount of energy carried by convection (and radiation) with an appropriate theory.

Despite the great importance of convection in modelling the structure and evolution of a star, a satisfactory treatment of stellar convection is still open to debate and until now a self-consistent description of this important physical phenomenon has been missing. Reviews of the current state-of-art of the turbulent non-linear magnetodynamics knowledges in the stars (mostly in the sun) can be found in several books (e.g. Biskamp 1993; Somov 2006; Hughes, Rosner

★ E-mail: s.pasetto@ucl.ac.uk

& Weiss 2012). The goal has been to establish from basic physical principles a self-consistent description of convection represented by a group of equations with no ad hoc parameters.

In this context, the most successful theory of stellar convection in the literature is the mixing-length theory (ML theory). The ML theory stands on the works of Prandtl (1925), Biermann (1951), and Böhm-Vitense (1958). Thanks to the success it has achieved over decades of usage, it is considered as the reference paradigm to which any new theory has to be compared. In the ML theory, the motion of convective elements is expressed by means of the mean-free-path l_m that a generic convective element travels inside the convectively unstable regions of a star (e.g. Kippenhahn et al. 2012). l_m is assumed to be proportional to the natural distance scale h_p given by the pressure stratification of the star. The proportionality factor is called the ML parameter Λ_m, which is implicitly defined by the relation $l_m = \Lambda_m h_p$. Although this parameter must be determined with external arguments i.e. the calibration of the ML theory on observations of the Sun, the possible dependence on the star mass and evolutionary stage (their position in the HRD) can be neither excluded nor assessed. The ML parameter has a paramount importance in calculating the convective energy transport, and hence the radius and effective temperature which fix the trajectory of the stars in the HRD.

To overcome this situation, several approaches have been proposed in literature. The simplest one is the already mentioned fit of results obtained with a ML parameter to observations of different stars in the CMD. In alternative formulations allow the ML parameter to change with the position on the HRD (e.g. Pinheiro & Fernandes 2013). This approach is an extension of the original idea by Böhm-Vitense (1958) of the fit on the Sun. Helioseismology and/or asteroseismology (Brown & Gilliland 1994; Christensen-Dalsgaard 2002; Chaplin 2013; Chaplin & Miglio 2013) and much better data on the Sun produced by Solar Heliospheric Observatory (SOHO) offer independent ways of testing stellar convection and constraining the ML theory in turn (e.g. Ulrich & Rhodes 1977; Kueker, Ruediger & Kitchatinov 1993; Grossman 1996).

Recently, sophisticated fully 3D-hydrodynamic simulations have been used to model and test convection. This approach requires large, time consuming computational facilities to integrate the 3D-Navier–Stokes equations (e.g. Ludwig, Jordan & Steffen 1994; Bazán & Arnett 1998; Ludwig, Freytag & Steffen 1999; Brun & Toomre 2002; Meakin & Arnett 2007; Brown et al. 2008; Miesch et al. 2008; Brun, Miesch & Toomre 2011; Chiavassa et al. 2011; Collet, Magic & Asplund 2011; Augustson et al. 2012; Magic et al. 2013; Magic, Weiss & Asplund 2015; Salaris & Cassisi 2015).

The advantage here is that, unlike in the 1D integrations, parameter-free models of convection can be used. However, it has a very poor interpretative power: to extract a theoretical model from a simulation is not any simpler than writing a new one from scratch.

Finally, the third approach is to develop ML parameter free (or scale-free) theories by construction. It is worth mentioning, a few examples as Lydon, Fox & Sofia (1992), Balmforth (1992) or Canuto & Mazzitelli (1991) where nevertheless other free-parameters have been used instead of the ML. The turbulent scale-length in Canuto & Mazzitelli (1991) is the most popular case.

In a recent paper, Pasetto et al. (2014) developed the first theory of stellar convection that is fully self-consistent and scale-free. In this scale-free convection (SFC) theory, the convective elements can move radially and expand/contract at the same time, and, in addition to the buoyancy force, the inertia of the fluid displaced by the convective elements and the effect of their expansion on the buoyancy force itself are taken into account. The dynamical aspect

of the problem is formulated differently than in the classical ML theory, and the resulting equations are sufficient to determine the radiative and convective fluxes together with the medium and element temperature gradients, as well as the mean velocity and dimensions of the convective elements as a function of the environment physics (temperature, density, chemical composition, opacity, etc.), with no need of the ML parameter. Pasetto et al. (2014) applied the new theory to the case of the external layers of the best model representing the Sun calculated with the calibrated ML theory by Bertelli et al. (2008).

In this study, the SFC analysis is extended first to model atmospheres and then to exploratory stellar models calculated with the new theory. The results are similar to those based on the classical ML theory.

The plan of the paper is the following. In Section 2 we briefly present the schematic structure as it is relevant for our study. In Section 3 we summarize our treatment of stellar convection as presented in Pasetto et al. (2014). In Section 4 we present the solution of the stellar equation that we are going to adopt. In Section 5 we treat the boundary condition for the convective outer layers of the stars. In Section 6 we present some application to the first stellar model of our theory. In Section 7 we comment on our results. In Appendix A we summarize the basic equations of stellar structure in the photosphere and atmosphere, together with a few key thermodynamical quantities concerning the equation of state (EoS) with ionization and radiation pressure. In the Appendix B, first we briefly review the classical ML theory with particular attention to the one we have used here and then present the key hypotheses, assumptions and results of the new SFC theory of Pasetto et al. (2014).

2 SCHEMATIC STRUCTURE OF A STAR

Three regions can be considered in the treatment of the physical structure of a star.

(i) The most external layers, i.e. the photosphere described by the optical depth, the bottom of which yields the surface of the star and determines the radius r_* and effective temperature $T_{\rm eff}$.

(ii) The atmosphere which extends downwards for about the 3–5 per cent in mass of the star, M_* from the bottom of the photosphere $\frac{M_{\rm atm}}{M_*} \in [1.0, 0.97/0.95[$ (with this notation we specifically refer to the outer layer in radius of the star, as opposite to the central part that would be indicated as, e.g. $\frac{M}{M_*} \in [0.1, 0.2[$). In the atmosphere the approximation of constant luminosity (i.e. without sources or sinks of energy) can be assumed, and light elements like H and He are partially ionized. Convection is far from the regime of $\nabla - \nabla_{\rm ad} \simeq 0$. In this region both the ML theory and SFC theory find their prime application.

(iii) The inner regions from $M_{\rm atm}$ to the centre in which energy production takes place, ionization of all elements such as H, He, C, N O etc. is complete and convection becomes adiabatic. This inner region of the stars can contain a convective envelope, extension of the convective region in the atmosphere but in which convection is nearly adiabatic. The convective envelope can extend quite deeply in the star. Stars in the mass range $M_* \in [0.3, 1.1[\,{\rm M_\odot}$ or so have a radiative core on the main-sequence, stars with $M_* \le 0.3\ {\rm M_\odot}$ are fully convective during their whole live. Stars more massive than about $M_* \ge 1.1/1.3\ {\rm M_\odot}$ develop a convective core from which convective overshooting can occur. Massive stars ($M_* \ge 10\ {\rm M_\odot}$) may develop intermediate convective shells in the post-main-sequences stages. All stars have convective cores during

the core- He burning phase and beyond (their occurrence depending on the star's mass).

The notation in use and the physical description of regions (i) and (ii) are as in the Göttingen stellar evolution code Hofmeister, Kippenhahn & Weigert (1964), the ancestor of the code used by Padova group for about five decades (see also below for more details). Details are given for the physical structure and mathematical technique used to calculate the physical variables in regions (i) and (ii) in the Appendix A. Specifically we present the basic equations for the photosphere and atmosphere, the treatment of ionization, and a few important thermodynamical quantities such as specific heat at constant pressure c_P, the ambient gradient ∇_{ad} and thermodynamical quantity Γ_1 for a gas in presence of radiation pressure and ionization that are needed to describe the super-adiabatic convection both in the ML and SFC theory.

Details on the main assumptions concerning the physical input of the equations describing region (iii), the treatment of convective overshooting from the core (if required) are given in Section 6.

3 THE SET OF EQUATIONS FOR THE SFC THEORY

The system of equations equation (60) as in Pasetto et al. (2014) must be solved to determine the convective/radiative-conductive transfer of energy in the photosphere and atmosphere of a star. They are well defined equations once the quantities $\{T, \kappa, \rho, \nabla_{\mathrm{rad}}, \nabla_{\mathrm{ad}}, g, c_p\}$ are considered as input and considered constant. These quantities are, respectively, the local averaged temperature of the star, interpolated opacity tables, averaged density of the star, the radiative gradient as in equation (A15), the adiabatic gradient as in equation (A23) in the appendix, gravity and heat capacity at constant pressure as in equation (A21), considered as quantities averaged over an infinitesimal region $\mathrm{d}r$ and time interval $\mathrm{d}t$. This means that the time-scale over which these quantities vary is supposed to be much larger than the time over which the results of the integration over the time of the system of equations for convection are achieved. Under these approximations, the system of equations proposed in Pasetto et al. (2014) is

$$
\begin{cases}
\varphi_{\mathrm{rad/cnd}} = \frac{4ac}{3} \frac{T^4}{\kappa h_p \rho} \nabla \\[2mm]
\varphi_{\mathrm{rad/cnd}} + \varphi_{\mathrm{cnv}} = \frac{4ac}{3} \frac{T^4}{\kappa h_p \rho} \nabla_{\mathrm{rad}} \\[2mm]
\frac{v^2}{\xi_e} = \frac{\nabla - \nabla_e - \frac{\varphi}{\delta} \nabla_\mu}{\frac{3h_p}{2\delta v_0 \tau} + \left(\nabla_e + 2\nabla - \frac{\varphi}{2\delta} \nabla_\mu\right)} g \\[2mm]
\varphi_{\mathrm{cnv}} = \frac{1}{2} \rho c_p T \left(\nabla - \nabla_e\right) \frac{v^2 t_0 \tau}{h_p} \\[2mm]
\frac{\nabla_e - \nabla_{\mathrm{ad}}}{\nabla - \nabla_e} = \frac{4acT^3}{\kappa \rho^2 c_p} \frac{t_0 \tau}{\xi_e^2} \\[2mm]
\xi_e = \left(\frac{t_0}{2}\right)^2 \frac{\nabla - \nabla_e - \frac{\varphi}{\delta} \nabla_\mu}{\frac{3h_p}{2\delta v_0 \tau} + \left(\nabla_e + 2\nabla - \frac{\varphi}{2\delta} \nabla_\mu\right)} g \chi(\tau),
\end{cases}
\tag{1}
$$

where $\varphi_{\mathrm{rad/cnd}}$ is the radiative/conductive flux, a the density-radiation constant, c the speed of light, T the local average temperature, κ the opacity, h_P the pressure scaleheight, ρ the star density, φ_{cnv} the convective flux, ξ_e the average size of the convective cell moving with a average velocity v, g the gravity, $\tau = \frac{t}{t_0}$ a normalized time and $\chi = \frac{\xi_e}{\xi_0}$ a normalized size of the convective elements. All these quantities are here treated as locally and temporally averaged. More details on the physical meaning of all the quantities are given in the Appendix B where a somehow different derivation of exactly these equations is explored and commented. The form taken by the above equations in the case of chemically homogeneous layers is

straightforwardly derived from setting $\nabla_\mu = 0$. Let us briefly comment each equation of equation (1) from (i) to (vi), highlighting the points of novelty with respect to the ML theory.

(i) and (ii) In this set of equations, the first two represent the radiative plus conductive fluxes $\varphi_{\mathrm{rad|cond}}$, and the total flux $\varphi_{\mathrm{rad|cond}} + \varphi_{\mathrm{conv}}$ which defines the fictitious radiative gradient ∇_{rad}.

(iii) The third equation introduces one of the new aspects of the theory: the average velocity of the convective elements at a given location within the stars. Compared to the ML theory the velocity is derived from the acceleration which in turn contains the inertia of the displaced fluid. The remarkable point of this equation is that for chemically homogeneous layers ($\nabla_\mu = 0$) it reduces to the equivalent in Schwarzschild approximation for stability against convection.

(iv) The fourth equation represents the convective flux. Although the overall formulation is the same as in the ML theory, here the velocity is corrected for the effects of the inertia of the displaced fluid. See also below for the discussion on the asymmetry of the velocity field.

(v) The fifth equation greatly differs from its analogue of the ML theory. It measures the radiative exchange of energy between the average convective element and the surrounding medium taking into account that convective elements change their dimension, volume and area of the radiating surface as function of time because of their expansion/contraction. In this theory, the energy transfer is evaluated at each instant whereas in the classical ML theory the mean size, volume and area of the emitting surface of the convective elements are kept constant. The dependence of the energy feedback of the convective element with its surrounding is the heart of this description of convection processes.

(vi) The last equation yields the mean size of the convective elements as a function of time. Its presence is particularly important because it replaces the ML theory assumption about the dimension of the convective elements and also the distance travelled by these during their lifetime. This equation achieves the closure of the system of equations.

In the following subsection we will comment on a few aspects of the SFC theory.

3.1 Time dependence and uniqueness theorem

The system of equations equation (1) and its solution contain the time. Therefore one may argue that the ML, free parameter of the ML theory, is now replaced by the time and that there is real no advantage with the new theory of convection but for a better description of the dynamics. Furthermore, there are six degrees of freedom over six unknowns instead of the five degrees of freedom plus one free-constant over five unknowns of ML theory equation (B1). The solution of this apparent problem is achieved by the Uniqueness Theorem. Pasetto et al. (2014) have rigorously demonstrated that the ratio $\chi/\tau^2 \to$ const as the time grows and the solutions of the system of equations (1) have to be searched in the manifold described by

$$
\frac{(\nabla - \nabla_e)^2}{(\nabla_{\mathrm{rad}} - \nabla)(\nabla_e - \nabla_{\mathrm{ad}})} = \text{const.}
\tag{2}
$$

When the solutions enter the regime $\chi/\tau^2 \to$ const where the Uniqueness theorem holds, we simply speak of an 'asymptotic regime' for the solutions. This equation describes a surface containing the manifold of all possible solutions. By assigning ∇_{rad} and ∇_{ad} at each layer within a star, ∇ and ∇_e are asymptotically

related by a unique relation. There is no arbitrary scalelength to be fixed. This theorem proves that, to the first order, there exists an unique manifold solution of the system equation (1). The evolution of the system is forced to stay in a single time-independent manifold by the relation existing between the evolution of the average size of the convective elements and the environment where the convective elements are embedded. This relation holds only in the subsonic regime, but in such a case it is completely general.[1] In our context it implies that the temporal evolution of the system equation (1) has to cancel out: an asymptotic behaviour of the physical variables must exist. The time variable is needed to know when the asymptotic regime is reached by the system and the theory becomes fully applicable. The Uniqueness Theorem 'de-facto' closes the equations and rules out the need of the ML free parameter.

3.2 Comoving reference frame S_1

The advantage of an analysis made in a comoving reference frame centred on the convective element can be captured with these simple arguments. We consider the kinetic energy associated with a convective element in the reference system $S_0(O; x)$ not comoving with the element. From the equation of the potential flow (e.g. equation B8), putting at rest the flow far away from the bubble (i.e. adding a flux $\langle v, x \rangle$) we can obtain $E_k = \frac{1}{2}\rho \int_V \|v\|^2 d^3x = \frac{\pi}{3}\rho \xi_e^3 \left(6\dot{\xi}_e^2 + v^2\right)$. Here the spatial or temporal averages for the quantities $\bar{\xi}_e, \bar{v}, ...$ are omitted but they are implicitly taken into account. For the potential energy, excluding the contribution of the surface tension as mentioned above, we can write simply write $E_p = E_p(\xi_e, P^\infty) + \Phi_g$, i.e. the potential energy is the sum of the potential energy of the fluid $E_p(\xi_e, P^\infty)$ (that in S_0 is a function of the size of the convective element and of the pressure far away from the bubble) and the gravitational potential of the star. If we limit ourselves to the equations of motion (EoM) for the radial direction outside the stars, r, the EoM is

$$\begin{cases} \frac{d}{dt}\left(\frac{\partial L}{\partial \dot{\xi}_e}\right) - \frac{\partial L}{\partial \xi_e} = 0 \\ \frac{d}{dt}\left(\frac{\partial L}{\partial \dot{r}}\right) - \frac{\partial L}{\partial r} = 0 \end{cases} \Leftrightarrow \begin{cases} \frac{3}{2}\dot{\xi}_e^2 + \ddot{\xi}_e\xi_e - \frac{P(\xi_e) - P^\infty}{\rho} = 0 \\ A = 2g, \end{cases}$$

(3)

with L the Lagrangian of the system. Thanks to the Lagrangian formalism, knowing the explicit formulation for $E_p(\xi_e, P^\infty)$ is not necessary, because it satisfies the equation $E_p(\xi_e, P^\infty) = -\int_V (P(\xi_e) - P^\infty) d^3x$. With the aid of the equation for hydrostatic equilibrium we re-obtain equation (B11) of the first Theorem in Pasetto et al. (2014) but without the term containing the acceleration A (or with $A = 0$) that provides the dynamical coupling between S_0 and S_1. This forced us to apply directly the Lagrangian formalism to non-inertial reference frames as already done by Pasetto & Chiosi (2009, section 3.1) in a different context (see also Landau & Lifshitz 1969, section 39 for the point mass approximation). Finally, we note how this suggests also a different, completely independent derivation of the main theorem of section 4.1 of Pasetto et al. (2014) from a Lagrangian formalism.
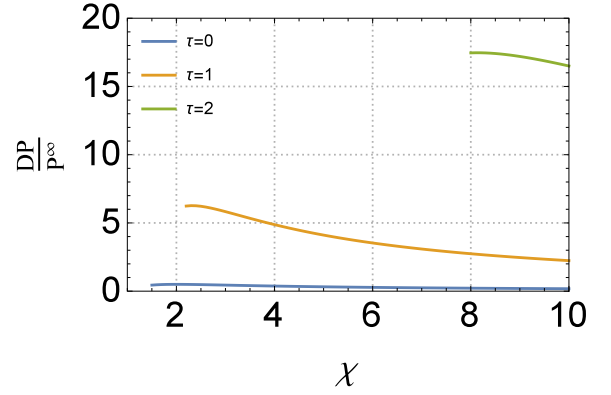
Figure 1. Evolution with the time of the pressure difference DP/P^∞ at the surface of a generic convective element. The time necessary to reach the pressure equilibrium is not null, and the equilibrium it is reached only 'far away' form the surface of the convective element. A convective element cannot exist at all, if it is assumed to be always in perfect mechanical equilibrium with the environment.

3.3 Local departure from hydrostatic equilibrium

The SFC theory of convection is based on the assumption of non-local pressure equilibrium and hence local deviations from rigorous hydrostatic equilibrium (a situation therein-after referred to as mechanical equilibrium), i.e. the stellar plasma is not in mechanical equilibrium on the surface of the expanding/contracting convective element while this latter is moving outwards/inwards. A convective element coming into existence for whatever reason and expanding into the medium represents a perturbation of local pressure that cannot instantaneously recover the mechanical equilibrium (pressure balance) with the surrounding. The condition of rigorous mechanical equilibrium with the stellar medium is met only 'far away' from the surface of a convective element, i.e. only in the limit $\xi_e \to \infty$.

In many textbooks of stellar astrophysics (e.g. Cox & Giuli 1968; Kippenhahn et al. 2012), the simple assumption of instantaneous pressure equilibrium is made because of the high value of the sound speed. Indicating the pressure difference between the element (at the surface) and medium as $DP \equiv P - P^\infty$, it is generally assumed $DP = 0$ identically. This is clearly a wrong assumption if one needs to argue about local deviations from hydrostatic equilibrium. There exists no instantaneous pressure equilibrium. No matter how fast it is reached, the sound speed is not infinite. We take advantage of the equation (3) (which is a particular case of theorem of section 4.1 in Pasetto et al. (2014)) to demonstrate this. In Fig. 1, we show the temporal behaviour of the ratio DP/P^∞ derived from the first Lagrangian equation of System equation (3) using, e.g. for the temporal evolution of ξ_e an arbitrary relation of the type $\xi_e \propto \tau^2$. As evident from Fig. 1, only far away from the convective element $\frac{P}{P^\infty} \to 1$, i.e. $\frac{DP}{P^\infty} \to 0 \, \forall \tau$. Note that the potential flow approximation, the assumption of irrotational fluid (no vorticity), and the evolution (increase/decrease) of the surface of a convective element predicted by our theory (see Sections B2.2 and B2.3), all act to determine the long range behaviour of the pressure perturbation. In a fluid with null vorticity, the pressure perturbation scales as $O\left(\xi_e^{-1}\right)$, the case shown in Fig. 1. In a fluid with non-zero vorticity the pressure perturbation is expected to scale with the distance as $O\left(\xi_e^{-3}\right)$ (e.g. Batchelor 2000). This should leave detectable traces at the small wave-numbers, k, end of the energy spectrum, $E(k)$, which is known to be heavily dependent on the long range behaviour. A direct comparison of this issue with numerical simulations is left for future investigations (Pasetto et al., in preparation). Even though the

theory does not require the mechanical equilibrium for the convective element, because the star as a whole is in hydrostatic equilibrium the condition is also formally met for the equation of convection, but only far away from the surface of the convective element. However, by 'far away' we mean always a distance close enough so that the local density has remained nearly constant. This description of the physical situation as far as the mechanical equilibrium at the surface of a convective element is concerned agrees with current understanding of fluid dynamics (Landau & Lifshitz 1959; Batchelor 2000) and the current more approximate assumption made by the classical ML theory that convective elements expand/contract in mechanical equilibrium with the surroundings.

3.4 Surface tension on convective elements

It is worth recalling here that in the SFC theory no physical surface is enclosing a convective element and therefore the Young–Laplace treatment of the surface tension is not applied. This approach differs from classical literature on fluids in which the surface tension is taken into account (e.g. Tuteja et al. 2010, and reference therein). Our approach is consistent with astrophysical 3D-hydrodynamical simulations where convection is represented by small volumes moving up and down for a short time, not surviving long enough for surface tensions to be relevant.

3.5 More general remarks: strength and weakness of the SFC theory

In addition to be above issues, we would like to shortly comment here on points of strength and weakness of the SFC theory that deserve further investigation.

Since the early studies of Boussinesq (1870), Prandtl (1925) and on the Reynolds stress model, the closure of the hierarchy of averaged moment equations represented a formidable challenge for the description of turbulence and convection. Despite its simplicity, our model represents the first and to date unique way to close the equation of stellar convection, without any arbitrarily free assumptions. It is fully analytical: neither ad hoc fitting on HRD stars nor numerical simulations are required to find closure of the equations. Furthermore, rotation can be implemented in a simple fashion because the formalism of accelerated reference frames of type S_1 is already *in situ*.

Up to now only few points of weakness have been identified. First of all, the SFC theory is a linear theory. Therefore it cannot deal with nonlinear phenomena that would require higher order expansion over $\varepsilon \equiv \frac{|v|}{|\xi_e|} \ll 1$ and a suitable treatment of resonances. This problem has not been investigated yet in the context of this theory for the stellar plasma but it may have strong physical implications. The uniqueness theorem that provides the closure of the stellar equation does not hold in the non-linear regime. Hence, we expect that second-order effects will require further free parameters, as it was the case of the ML theory, to reach a finer physical description.

Closely related to the previous problem is the determination of the distribution function of the size of the convective cells. The distribution function of a turbulent cascade of eddies is not Gaussian. In our study, we consider only with the first-order moments of the unknown underlying distribution function. This approach is far from being a correct description of the reality. However, even if the number of underlying moments required to map correctly the distribution function and hence the nature of the convection within the stars is very high, it is not infinite (see e.g. Cubarsi 2010).

The sizes of the convection cells are expected to span from large integral scales containing the most of the kinetic energy in

an anisotropic motion down to the Kolmogorov's micro-scales of the small eddies with randomly isotropic motion where the viscous forces are effective (at least for high Reynold numbers). For the sake of simplicity, dealing with the stellar plasmas, we limit ourselves to a treatment favouring the self-consistency to the complexity.[2]

Finally, by construction, this SFC theory does not suitably describe the border regions of convective zones where convective cells could overshoot from the Schwarzschild border into the surrounding radiative regions. This is possible only suitably modifying this SFC theory (Pasetto et al., in preparation).

Based on the results that we are going to present here, we are confident that some of the above criticisms will be found to be unimportant. Indeed, we will find in what follows that the first stellar models, with the envelope convection treated according to the Pasetto et al. (2014) theory are similar to those derived from the best tuned ML theory. We will return to the implications of these results in relation with the above criticisms in Section 7.

3.6 Direct numerical and large eddy simulations

Before introducing the mathematical and numerical method we have adopted to solve the system of equations (1), it is worth discussing briefly numerical techniques for solving the Navier–Stokes equations.

1D numerical simulations are suitably and successfully designed to generate large grids of stellar models, evolutionary tracks and isochrones, to quickly map the whole HRD, and to compare model results with observational data. Thanks to the 1D formalism, the physics of stellar structure and evolution is one of the best known area of astrophysics. 1D solutions are still worth being pursued in order to test the self-consistency of the SFC theory and to highlight the advantages it offers with respect to the classical ML theory. Nevertheless, nowadays models based on the full 3D formalism are becoming more and more common and important in astrophysics and it would be worth comparing the results of our 1D SFC theory with some of these 3D numerical solutions of Navier-Stokes based on direct numerical (DNS) or Large-Eddy (LES) schemes. However, to provide a direct comparison requires these solutions to be tailored specifically with this test in mind. None are immediately available, hence we leave such a comparison to future investigations, and in Section 6 we limit ourselves to a quick comparison of some of our results with those from full 3D simulations.

The numerical integration of partial differential equations (PDE) has a long story, even if the integration schemes of the Navier–Stokes equations of convection are relatively recent (see the review by Glatzmaier 2013). The major advantage in using numerical simulations of stellar convection is that no closure schemes are required as in most analytical treatments and that the entire spectrum of the sizes of convective elements (at least in principle in the DNS) can be considered. For comparison, our approach deals only with average quantities, i.e. equation (1) refers only to the first-order moments of an underlying (unknown) distribution of the sizes of convective elements. Therefore, at this stage of the SFC theory we are still missing the redistribution of the energy down to the cascade of convective cells that in contrast can be followed with fully hydrodynamical simulations. However, remarkably, from numerical and observational experiments it is well known that the majority of the kinetic energy in convective transport is contained in the larger convective elements and that the convection reaches a 'fully developed' state

---

[2] Concerning the chaotic versus turbulent nature of the inertia term that we retained in the Navier–Stokes equations see, e.g. Ottino (1989).

after some time, a behaviour that recall the *asymptotic behaviour* evidenced in our analytical solution.

Moreover, the treatment of the fully hydrodynamic even equations in 3D schemes is not free of limitations. Drawbacks of the DNS are the resolutions and the computational time. From the early studies of Orszag (e.g. Orszag 1971; Orszag & Patterson 1972), where the Reynold numbers (based on the Taylor microscale) were of the order $\Re_\lambda \sim 35$, we today have simulations with $\Re_\lambda \sim 800/1000$ on average (e.g. Ishihara et al. 2007). Even so, this hampers the applicability of DNS to stellar cases, owing to the very high $\Re \sim 0.02\Re_\lambda^2 > 10^{10}$, because the number of data points N, scales with the number of degrees of freedom of the turbulence, $\Re^{9/4}$ (Landau & Lifshitz 1959) as $N^3 \sim \left(\frac{L_{\mathrm{grid}}}{\ell}\right)^3 \Re^{9/4}$, and hence the computational time becomes exceedingly long. All this imposes a limit to the spatial scale L_{grid} to a few Kolmogorov integral scales, say $L_{\mathrm{grid}} \sim 5\ell$. Pseudospectral methods in the LES formalism and spherical symmetric geometry can improve the situation, but only partially (e.g. Brun & Toomre 2002; Canuto et al. 2006). The success of the LES approach relies on the fact that energy tends to travel downwards the energy cascade, from large to small scale convective elements. These latter are finally cut off by residual-stresses and viscosity so that the large scales *should not know* about the absence of the small ones.

The potential offered by the LES scheme has been amply demonstrated; for instance, it has been successfully used in combination with the anelastic spherical harmonics solver with increasing degree of complexity in several studies of solar physics (e.g. Brown et al. 2008; Brun et al. 2011; Augustson et al. 2012) where rotation, tachocline and compressibility of the fluid are taken into account. LES is also suited to interpret results from a first-order-moment system like that in equation (1). LES's main limitations are mostly related to periodicities such as those generated by fake anisotropies or long-range correlations (e.g. Ishihara, Gotoh & Kaneda 2009; Kenada & Morishita 2014; Jimenez & Kawahara 2014, for a review).

Aware of the limitations implicit in our theory represented by equation (1) when compared with full 3D hydrodynamic simulations, we present in the section below the method we have adopted to solve the basic equations of the SFC theory. Then, instead of undertaking a detailed comparison of the results with those from LES, we proceed to calculate full stellar models and evolutionary tracks based on the SFC theory (see Section 6) and show that the new stellar models directly agree with those based on the classical ML theory and that 1D-based models can fairly agree with the data of real stars which is the goal of this work.

4 SOLVING THE BASIC EQUATIONS

We present an algebraic numerical procedure to solve the system of equation (1). Following Pasetto et al. (2014) we assume $g_4 = \frac{g}{4}$ and $\alpha = \frac{acT^3}{\kappa\rho^2 c_p}$ where all the symbols have their usual meaning and we limit ourself to the homogeneous case $\nabla_\mu = 0$. Inserting the first of equations (1) into the second, and performing a number of algebraic manipulations, the system equation (1) rapidly reduces to this set of four equations in four unknowns:

$$
\begin{cases}
v^2 = \frac{4g_4\xi_e(\nabla-\nabla_e)}{\frac{3h_p}{2\delta v\tau}+2\nabla+\nabla_e} \\
\frac{4\alpha(\nabla_{\mathrm{rad}}-\nabla)}{3h_p} = \frac{v^2 t_0\tau(\nabla-\nabla_e)}{h_p} \\
\frac{\nabla_e-\nabla_{\mathrm{ad}}}{\nabla-\nabla_e} = \frac{4\alpha\tau}{\xi_e^2} \\
\xi_e = \frac{g_4\chi(\nabla-\nabla_e)}{\frac{3h_p}{2\delta v\tau}+2\nabla+\nabla_e}.
\end{cases}
\tag{4}
$$

There are several different techniques for finding the solutions of the system equation (4). In what follows we limit ourselves to present the most stable of these solutions from a algebraic/numerical point of view.

From the second equation of system equation (4) we isolate the gradient of the convective elements:

$$
\nabla_e = \frac{4\alpha(\nabla-\nabla_{\mathrm{rad}})}{3v^2 t_0\tau} + \nabla,
\tag{5}
$$

and insert it into the other equations of system equation (4) to obtain

$$
\begin{cases}
v^2 = \frac{32\alpha\delta g_4\xi_e(\nabla_{\mathrm{rad}}-\nabla)}{2\delta\nabla(4\alpha+9v^2 t_0\tau)+9vh_p t_0-8\alpha\delta\nabla_{\mathrm{rad}}} \\
\frac{3v^2 t_0\tau(\nabla_{\mathrm{ad}}-\nabla)}{4\alpha(\nabla-\nabla_{\mathrm{rad}})} = \frac{4\alpha\tau}{\xi_e^2}+1 \\
\xi_e = \frac{8\alpha\delta g_4\chi(\nabla_{\mathrm{rad}}-\nabla)}{2\delta\nabla(4\alpha+9v^2 t_0\tau)+9vh_p t_0-8\alpha\delta\nabla_{\mathrm{rad}}}.
\end{cases}
\tag{6}
$$

We proceed further by extracting the ambient gradient from the first of the previous equations:

$$
\nabla = \frac{8\alpha\delta\nabla_{\mathrm{rad}}\left(v^2+4g_4\xi_e\right)-9v^3 h_p t_0}{18\delta v^4 t_0\tau+8\alpha\delta\left(v^2+4g_4\xi_e\right)},
\tag{7}
$$

and introduce it into the remaining two equations to obtain a simple equation, that relates ξ and v:

$$
4\xi_e = \frac{v^2\chi}{\xi_e},
\tag{8}
$$

and a more complicated equation that relates all the other quantities:

$$
\begin{aligned}
&-9v^3 h_p t_0 - 8\alpha\delta\nabla_{rad}\left(v^2+4g_4\xi_e\right) \\
&+2\delta\nabla_{ad}\left(9v^4 t_0\tau+4\alpha\left(v^2+4g_4\xi_e\right)\right) \\
&= \left(\frac{4\alpha\tau}{\xi_e^2}+1\right)\frac{12\alpha v(2\delta v\nabla_{rad}\tau+h_p)}{\tau}.
\end{aligned}
\tag{9}
$$

The first of these equations, equation (8), offers an immediate solution for the size and/or velocity of a convective element. Once equation (8) is inserted in equation (9) we obtain a quintic equation in ξ_e (the current size of a convective element in S_1). At this point, we are tempted to exploit the fact that by construction ξ_e is always positive, and search for real positive solutions of the quintic equation in ξ_e:

$$
\sum_{i=0}^{5} c_i\xi_e^i = 0
$$
$$
\begin{cases}
c_5 = 1 \\
c_4 = \frac{\pm h_P\sqrt{\chi}}{4\delta\nabla_{\mathrm{ad}}\tau} \\
c_3 = \frac{\alpha t_0\chi(\nabla_{\mathrm{ad}}+2\nabla_{\mathrm{rad}})}{9\nabla_{\mathrm{ad}}\tau} \\
c_2 = \frac{12\alpha\pm h_P t_0\chi^{3/2}+\alpha\delta g_4 t_0^3\tau\chi^2(\nabla_{\mathrm{ad}}-\nabla_{\mathrm{rad}})}{144\delta\nabla_{\mathrm{ad}}\tau^2} \\
c_1 = \frac{4\alpha^2 t_0^2\nabla_{\mathrm{rad}}\chi}{3\nabla_{\mathrm{ad}}} \\
c_0 = \pm\frac{\alpha^2 h_P t_0^2\chi^{3/2}}{3\delta\nabla_{\mathrm{ad}}\tau},
\end{cases}
\tag{10}
$$

where $c_i \in \mathbb{R}_0^+$, $i = 1, ..., 5$ and $\xi_e \in \mathbb{R}_0^+$. Nevertheless this apparent advantage is not so helpful in practice. The solution of a quintic equation represents a formidable problem that kept occupied the most eminent minds of the past centuries and only in the 19th century a solution formula in terms of ultraradicals (elliptic functions) has been found (connection with icosahedral symmetry, King 2008). The implementation of this technique, despite offering a general analysis of equation (10), is beyond the goal of this paper.

We are mostly focusing on the impact and physical meaning of the convection equation (4) for the stars and on validating our theory. To this aim, we make use of physical assumptions and the theorem of uniqueness in Pasetto et al. (2014) to reach a comprehensive interpretation of our system. Hence, we omit to develop a complete mathematical treatment of the quintic equation (10) and proceed with the following arguments.

The average size of the convective elements is in bijective relation with the time (see Pasetto et al. (2014) appendix A, fig. A1). Our theory is valid only after some time interval has elapsed since the birth of a convective element (the time interval is however small compared to any typical evolutionary time-scale of a star). Similar considerations apply to the size of a convective element. Therefore both τ and ξ_e represent equally useful (unbounded) independent variables over which to solve our equations. The theorem of uniqueness proved that the system equation (1) has to develop an asymptotic behaviour for the independent variables and hence, e.g. on the velocity v too.

Because a quintic equation has solutions only in terms of ultraradicals, we find more convenient first to express the quintic equation in terms of v and then to operate numerically to solve it. The advantage and simplicity in determining numerically an asymptotic velocity v overwhelms in the practice the utility of the positive nature of ξ_e. Hence, we here propose to replace in equation (8) the variable ξ_e with the variable v to obtain the quintic as function of v (where positive and negative solutions have to be investigated). From equation (8) we get ($\chi > 0$ and $\xi_e > 0$, see also Appendix B):

$$\xi_e = \frac{|v|\sqrt{\chi}}{2}, \tag{11}$$

so that the system equation (4) reduces to

$$\sum_{i=0}^{5} c_i v^i = 0$$

$$\begin{cases} c_5 = 1 \\ c_4 = \frac{h_P}{2\delta t_0 \nabla_{ad}\tau} \\ c_3 = \frac{4\alpha(\nabla_{ad}+2\nabla_{rad})}{9t_0\nabla_{ad}\tau} \\ c_2 = -\frac{\alpha(\pm\delta g_4 t_0^2\tau\sqrt{\chi}(\nabla_{rad}-\nabla_{ad})-12h_P)}{18\delta t_0^2\nabla_{ad}\tau^2} \\ c_1 = \frac{64\alpha^2\nabla_{rad}}{3t_0^2\nabla_{ad}\chi} \\ c_0 = \frac{32\alpha^2 h_P}{3\delta t_0^3\nabla_{ad}\tau\chi}. \end{cases} \tag{12}$$

Owing to the odd velocity dependence of equation (12), the theory predicts different average velocities for up/down motions of convective elements. This effect has been already observed in numerical simulations (e.g. Arnett et al. 2015) and here now evident in our fully analytical treatment. The implication of this effect will be examined in greater detail in a forthcoming paper (Pasetto et al., in preparation) where over/under-shooting of the convective elements will be investigated.

Therefore, at each layer of the convective regions (which means at assigned input physics: density, temperature, etc.) the time has to be changed until the so-called asymptotic regime is reached (see Section 3). The time scanning is made according to the relation $t = 10^{e+\Delta e}$ [s] where, e.g. $e = 1, 2, ..., 15$ in steps of Δe. Δe is suitably chosen according to the desired time space and accuracy. Typical values $\Delta e \in [0.01, 0.05]$ produce fine resolution for the purpose of our work. At each time step $\hat{t}$ the integration of the quintic of equation (12) is performed with robust numerical algorithm (Jenkins & Traub 1970) and with the solution meeting the conditions

$$\begin{cases} \text{Im}\,[v] = 0 \\ \xi_e(\hat{t}) > \xi_e(\hat{t} - dt) \\ v(\hat{t}) > v(\hat{t} - dt) \\ \frac{v(\hat{t}-dt)}{v(\hat{t})} > \Pi, \end{cases} \tag{13}$$

where Π is a suitable percentage of the asymptote reached, for instance 98 per cent (i.e. $\Pi = 0.98$ in our notation). When this occurs, the velocity has reached its asymptotic value and the solutions are determined.

When the velocity v of a typical convective element is known, one can immediately calculate its dimension ξ_e and temperature gradient ∇_e, the temperature gradient of the medium ∇, the convective flux φ_{cnv}, and finally the radiative flux $\varphi_{rad|cnd}$. As the quintic equation contains the integration time τ, all these quantities vary with time until they reach their asymptotic value. Furthermore, at each time the quintic equation has solutions of which only those with null imaginary part have physical meaning and only those satisfying all the selection criteria equation (13) have to be considered. To illustrate the point, we take a certain layer located somewhat inside the external convective zone. The layer is at the inner edge of the super-adiabatic zone and it characterized by the following values of the physical quantities $R = 6.067\,36 \times 10^8$ m, $T = 6.295\,06 \times 10^3$ K, $P = 1.485\,94 \times 10^4$ Newton m^{-2}, $\rho = 3.630\,78 \times 10^{-4}$ kg m^{-3}, $\kappa = 9.671\,64 \times 10^{-2}$ m^2 kg^{-1}, $\nabla_{ad} = 0.384$, $\nabla_{rad} = 0.503$, and $\mu = 1.279$, solve the quintic equation and derive the whole set of unknowns listed above as a function of time until they reach the asymptotic value. The results are shown in Fig. 2 limited to the convective flux φ_{cnv} (left-hand panel) and ambient temperature gradient ∇ (right-hand panel). In this figure we display all the physical solutions, i.e. with Im[v] = 0. These are indicated by the green dots. Looking at the left-hand panel, at increasing time the number of real solutions varies from one to five and past 10^4 s to three and asymptotically only two. Similar trend is shown by the plot in the right-hand panel. The same quantities can also be obtained from the classical ML theory using the equations presented in Section B1. In this case only one real solution exists at each time. This is indicated by the black dots in both panels. Finally, of all the solutions given by the SFC theory only one is filtered by the selection criteria, i.e. the one with the highest value of φ_{cnv} and ∇. Therefore, in this layer the asymptotic value of the SFC theory solution is the same as that of the ML theory.

Is this situation the same for all layers of the convective zone? It answer is no, the SFC theory differs from the ML theory in the outermost regions, whereas it closely resembles the ML theory going deeper and deeper inside. The issue is examined in detail below.

5 SFC THEORY VERSUS ML THEORY ON THE SURFACE BOUNDARY CONDITIONS

The luminosity and effective temperature of a star of mass M_* and chemical composition [X, Y, Z] depend on the energy production (the luminosity) and the energy transport (the effective temperature). The latter, in turn, depends on the combined effect of the radiative and convective transport in the stellar atmosphere, and the very outer layers of this in particular.
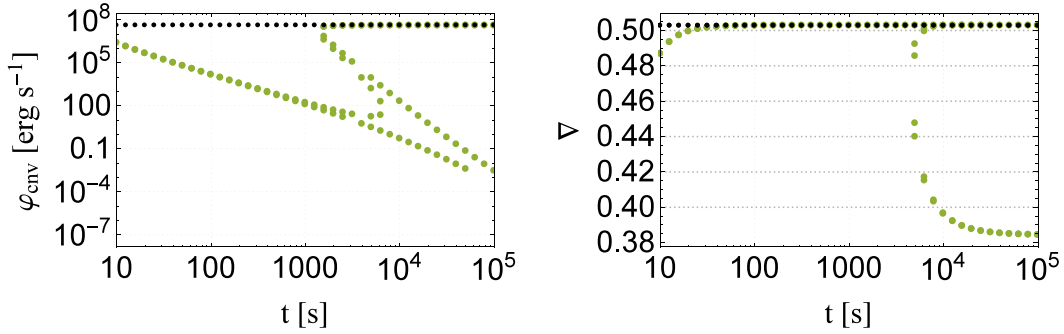
Figure 2. Convective flux (left-hand panel) and temperature gradient ∇ of the ambient medium (right-hand panel) as a function of time for a layer in the outer convective zone of the main-sequence model of the 1 M$_\odot$ star with chemical composition [$X = 0.703, Y = 0.280, Z = 0.017$]. In the two panels, we show the solutions from the quintic equation (12) of the SFC theory with their multiplicity (green dots) and the corresponding ones from the ML theory (black dots) with parameter $\Lambda_m = 1.68$. For times longer than a few 10^4 s one of the solutions from the SFC theory almost coincides with that from the ML theory. This layer falls at the inner edge of the region with strong super-adiabaticity.
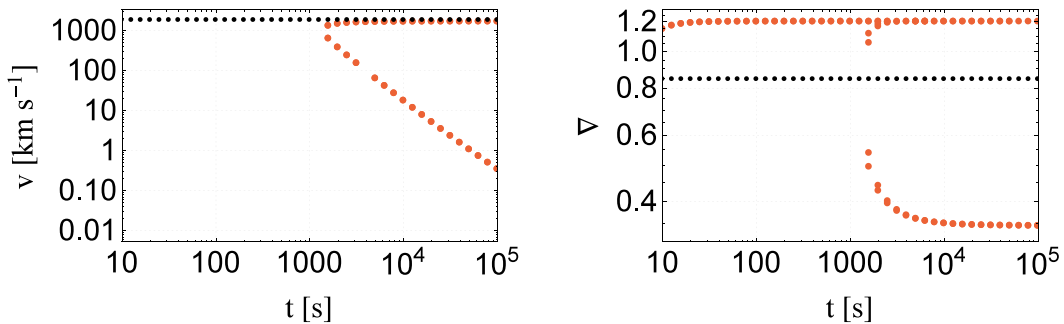

Figure 3. Similar to Fig. 2 but for the velocity (left-hand panel) and the ambient temperature gradient ∇ (right-hand panel) and for a different layer of the outer convective zone of the 1 M$_\odot$ with composition [$X = 0.703, Y = 0.280, Z = 0.017$] on the main sequence. This layer is below the photosphere but above the region of very strong super-adiabaticity. The physical units and the meaning of the symbols are the same as in Fig. 2. The degree of super-adiabaticity is larger that in Fig. 2. While the large values of the velocities from the SFC theory coincide with those from the ML theory for times longer that few 10^3 s, the temperature gradient does not.

What is the behaviour of the SFC theory at this external boundary condition and how to treat it? The theory developed is fully dynamical, i.e. it includes explicitly the time. Hence careful boundary conditions have to be accommodated to avoid to apply the theory where it loses physical significance, i.e. every time the evolution does not reach the 'asymptotic regime'. In the very external layers, a convective elements cannot travel and/or expand upwards beyond the surface of the star. This greatly reduces the dimension and velocity and lifetime in turn of an element that came into existence close to the star surface. Therefore it is likely that close to surface, the maximum time allowed to an element is shorter than the time required to reach the asymptotic values of all characteristic physical quantities of the element, the velocity in particular. As a side implication of these considerations, we expect that the resolution of the simulation, i.e. the mass and size zoning, number of mesh points etc. of the integration technique, should also play a key role in this issues. In other words, we expect a complex interplay between the mathematical and the numerical technique employed to simulate the stellar environment embedding the system equation (1) and the fundamental physics describing the intrinsically dynamical nature of the convection theory in use. This is expected also from the physical fact that the theory works on stellar layers not too large compared to spatial scale over which the gradients in the main quantities become relevant, but large enough to contain a number of convective elements well represented by statistical indicators (as mean, dispersion etc.). This con-

dition can possibly be missed at the boundary of the star (centre or surface).

The careful analysis of the outermost layers of stellar atmospheres reveals that while the values and profile of the velocity as a function of the position derived from the ML theory and SFC theory are nearly comparable, those for the ambient temperature gradient ∇ derived from the ML theory greatly differs from the corresponding ones obtained from the SFC theory. This is shown in Fig. 3 for one of external layers of the 1.0 M$_\odot$ with the chemical composition [$X = 0.703, Y = 0.280, Z = 0.017$] on the main sequence. The layer in question is located at the outer edge of the super-adiabatic zone and it is characterized by $R = 6.067\,36 \times 10^8$ m, $T = 7.194\,49 \times 10^3$ K, $P = 1.786\,49 \times 10^4$ N m^{-2}, $\rho = 3.819\,44 \times 10^{-4}$ kg m^{-3}, $\kappa = 3.258\,37 \times 10^{-1}$ m^2 kg^{-1}, $\nabla_{ad} = 0.345$, $\nabla_{rad} = 1.204$, and $\mu = 1.277$. As in Fig. 2, a very fine time spacing is adopted. Finally, the meaning of the symbols is the same as in Fig. 2. Also in this case we compare the SFC theory results with those from the ML theory. Looking at the velocity (left-hand panel), there is coincidence between the SFC theory and ML theory for the high value past the age of a few 10^3 s, whereas for ∇ at the time of a few 10^3 s, the solutions from the ML theory and the SFC theory show the minimum difference however without reaching coincidence, whereas they strongly deviate both for lower and higher values of the time (similar behaviour is found in other model atmospheres that are not shown here for the sake of brevity).
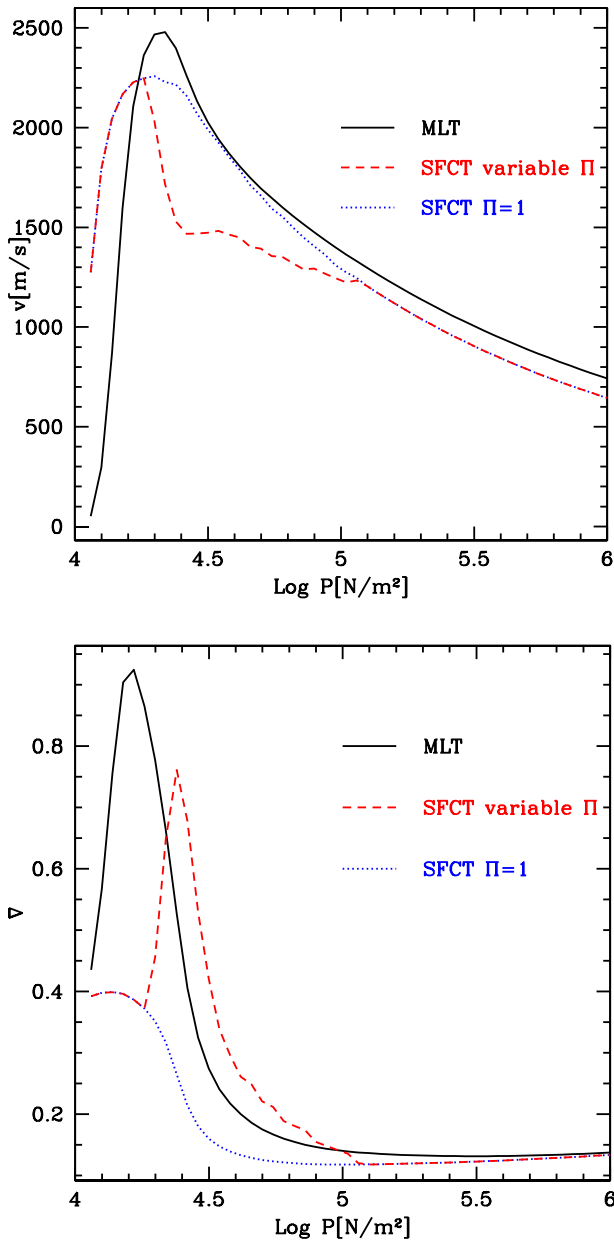
Figure 4. Top panel: the profile of the convective velocity as a function of the pressure across the atmosphere of the 1.0 M$_\odot$ star with initial chemical composition [$X = 0.703, Y = 0.280, Z = 0.017$], log$L/L_\odot = 0$ and age of about 4.6 Gyr, our best candidate to disposal that should fit the position of the Sun on the HRD. Three profiles are shown; the one derived from the ML theory (black solid line), the one derived from the SFC theory (blue dotted line) when the velocity at all layers is let reach the asymptotic regime ($\Pi = 1$ everywhere), and finally the third one (red dashed line) when the velocity in the outer layers can only reach a fraction of the asymptotic value ($\Pi < 1$ in the outer layers). Bottom panel: the same as in upper panel but for the temperature gradient ∇ of the medium.

To lend further support to the above results, we look at the systematic variation of both velocity and ambient temperature gradient across the external convective zone of the model with chemical composition [$X = 0.703, Y = 0.280, Z = 0.017$] and log$\frac{L}{L_\odot} = 0$ at the age of 4.6 Gyr, our best candidate to disposal to fit the position of the Sun on the HRD. The results are presented in Fig. 4 and are compared to those of the ML theory. The red solid lines show

the asymptotic velocity and companion ∇ derived from the straight application of the SFC theory. In the case of the ML theory (the black dots), the concept of an asymptotic regime for the velocity and ∇ in turn does not apply because given the physical condition of the medium there is only one, time-independent value for both the velocity and ∇. Velocities and temperature gradients in the deep regions of the convective zone predicted by the SFC theory and ML theory are nearly coincident whereas towards the surface they tend to greatly differ. The temperature gradients of the SFC theory is much lower than the one of the ML theory. Too low a value for the ambient ∇ would immediately imply a smaller radius and a higher effective temperature in turn (the luminosity being mainly driven by the internal physical conditions is hardly affected by what happens in the atmosphere). The immediate consequence is that the final position on the HRD of the evolutionary track is too blue to be able to match the Sun. Similar results are found also for models of star of different mass and evolutionary stage.

From this analysis, we learn that not all layers of a convective regions, those near the stellar surface in particular, can reach the asymptotic regime for the convective velocity (and also all other relevant quantities). To clarify this important issue, we proceed as follows.

We start calculating the time at which the solution of the quintic equation satisfies all the conditions of equation (13) (e.g. with $\Pi = 0.95$). This usually occurs when the time is about 10^5–10^6 s and sometime less in the outermost layers. We name this time 'numerical time t_{asy}'. It is not a physical time but a numerical-method dependent variable: different Π fixed arbitrarily give different t_{asy}. Then we argue that in a convective region, owing to continuous upward/downward motion of the fluid elements, the effect of any variation/perturbation of the physical quantities will soon or later propagate throughout the convective region at a speed whose maximum value is the sound speed $v_s = \sqrt{\Gamma_1 P/\rho}$ (with the usual meaning of all the symbols).[3]

Suppose now that the whole convective region has a width Δr_{cnv}. At each layer of the convective zone, we may calculate the sound velocity v_s and associate a temporal time-scale t_{cnv}, i.e. the time-scale a convective element would require to expand its size to the whole convective region. At each layer we have that the convective element expansion rate $\dot{\xi}_e \to v_s$ and the maximum size $\Delta\xi_e$ satisfies the condition $\Delta\xi_e = \Delta r_{cnv}/2$ so that we define t_{cnv} as

$$t_{cnv} \sim \frac{\Delta\xi_e}{\dot{\xi}_e} = \frac{\Delta\xi_e}{v_s} = \frac{\Delta r_{cnv}}{2v_s}. \tag{14}$$

At any layer the asymptotic regime cannot be reached if the two time-scales are in the ratio

$$\frac{t_{asy}}{t_{cnv}} = \Pi < 1. \tag{15}$$

This condition fixes also the maximum fraction of the local velocity with respect to its asymptotic value reached in each layer. The percentage Π varies with the position. Going deeper into the star the sound velocity increases, t_{cnv} decreases, and the condition (15) is always violated, i.e. the asymptotic velocity is reached anyhow. In these regions the ratio Π always reaches the maximum value $\Pi = 1$.

---

[3] It is worth noting here that since we are dealing we the most external layers in which the ionization of light elements (H,He, C, N, O, etc...) takes place, the expression for Γ_1 to use is the one containing the effect of ionization as well as radiation pressure. See appendix B or Cox & Giuli (1968) for details on the expression for Γ_1 we have used.
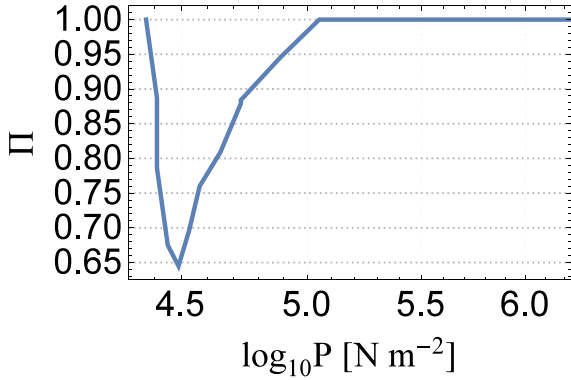
Figure 5. The profile of Π across the atmosphere of the MS model of the $1.0\,M_\odot$ star with chemical composition $[X = 0.703, Y = 0.280, Z = 0.017]$. Note the fall of Π to the minimum value followed by the rapid increase to $\Pi = 1$ at increasing pressure.

To illustrate the point, in Fig. 5 we show the profile of Π throughout the atmosphere of the zero age main-sequence model of the $1\,M_\odot$ star. It is worth noting that the asymptotic value of the velocity can be reached everywhere except in the outermost layers of the star for $\log P < 6\,\mathrm{N\,m^{-2}}$. As far as we can tell, this behaviour is the same in stellar models of the same mass but in different evolutionary stages and in models in the same evolutionary stage but different mass. Now we go back to the case of the stellar model representing the Sun and look at the velocity and ambient temperature gradient across the atmosphere when the condition equation (15) is applied. Now a profile Π similar but not identical to that of Fig. 5 is at work. The results are also plot in Fig. 4 (the red dashed lines in both panels). Now the profiles of velocity and ∇ in the outermost regions are much similar to those of the ML theory and therefore similar stellar models are expected (see Section 6).

From a technical point of view, the extent of the convective region Δr_{cnv} is not known a priori and therefore an iterative procedure must be adopted starting from a reasonable guess. Basing on the calculations of many model atmosphere, Δr_{cnv}, we expressed starting guess value for the convergence as $\Delta r_{conv} \simeq h_p \times N$, where h_p is the pressure scaleheight of the outermost layer and N the typical number of mesh points describing an atmosphere when $\log P$ is the independent variable. This finding greatly facilitates the task of choosing the initial guess for Δr_{cnv}. One or two iterations of the atmosphere are sufficient to refine Δr_{cnv} to the desired value. Our model atmospheres are calculated with $N \simeq 150$ mesh points. Using different codes with different resolving algorithm and numerical precision, different values of N can be found being this a limitation of the numerical integration scheme.

The procedure we have described acts as numerical scheme for the boundary conditions on the velocity profile in the outermost regions of a star. The number N of mesh points in the atmosphere is not a free parameter, but it is fixed by the mathematical technique and accuracy of the integration procedure (in our case $N \simeq 150$) and therefore it cannot be changed without changing these latter. Other stellar codes should have different values of N. However, limited to the following discussion we will take advantage of relations (14) and (15) to assess the model response to variations of Δr_{con}, Π, velocity v of the convective elements and finally ∇ by simply varying N. At each layer, keeping the sound velocity v_s constant (the physical quantities P, ρ etc. are assigned) lower Ns would imply smaller Δr_{cnv}, higher values of Π and velocity in turn, too low ∇s in outermost layers, and eventually too blue evolutionary
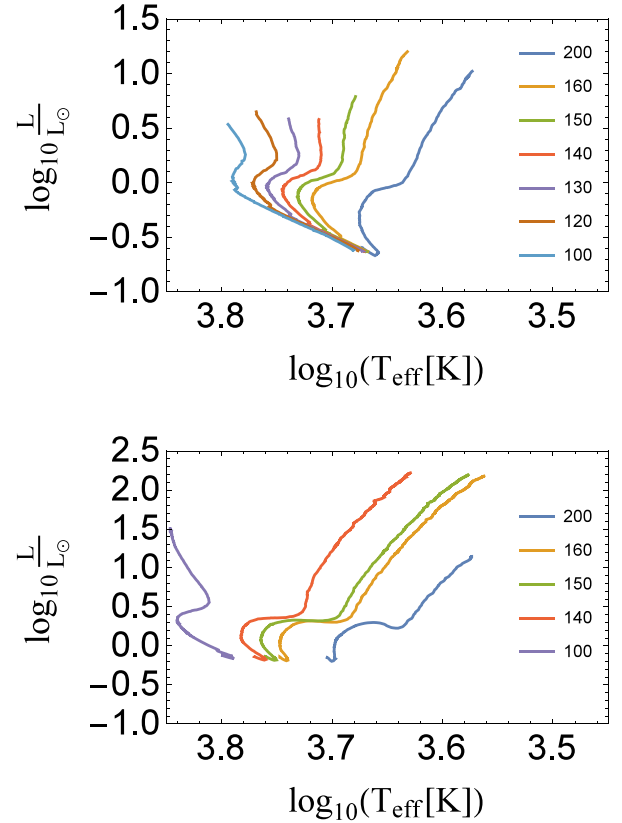

Figure 6. Evolutionary sequences of the $0.8\,M_\odot$ (top panel) and 1.0 $M_\odot$ (right-hand panel) stars with chemical composition $[X = 0.703, Y = 0.280, Z = 0.017]$ at artificially varying the number N of mesh points in the atmosphere as indicated. Only the case with $N = 150$ and the right value of Δr_{cnv} shows a track in agreement with current results in literature. The quintic is solved with time resolution $\Delta e = 0.01$. As explained in great detail in the text, low values of N correspond to small size of the convective region, high values of the velocity, smaller radii and hence higher effective temperatures. The opposite is the case of large values of N. Therefore only the correct Δr_{cnv}, profile Π, and velocities in the region of strong super-adiabaticity yield stellar models and evolutionary tracks in agreement with real HRDs. In other words, only the correct application of the SFC theory yields results able to reproduce the observations.

tracks in the HRD with respect to those from the ML theory. The opposite is the case for higher values of N. The results of these numerical experiments are shown in Fig. 6 for a test evolutionary sequences for the 0.8 and $1\,M_\odot$ with chemical composition $[X = 0.703, Y = 0.280, Z = 0.017]$, that are calculated forcing a variation of the size Δr_{cnv} by varying the number N as indicated. In conclusion, the correct physical description of the outermost layers of the external convective region of a star is crucial to calculate stellar models able to reproduce the position of real stars on the HRDs.

6 RESULTS

As already recalled in the previous sections, both the classical ML theory and the new SFC theory find their best application in the convective regions of the outer layers of a star where the super-adiabatic convection occurs. Therefore, first we investigate the physical structure of model atmospheres that are calculated both with the standard ML theory and the new SFC theory.
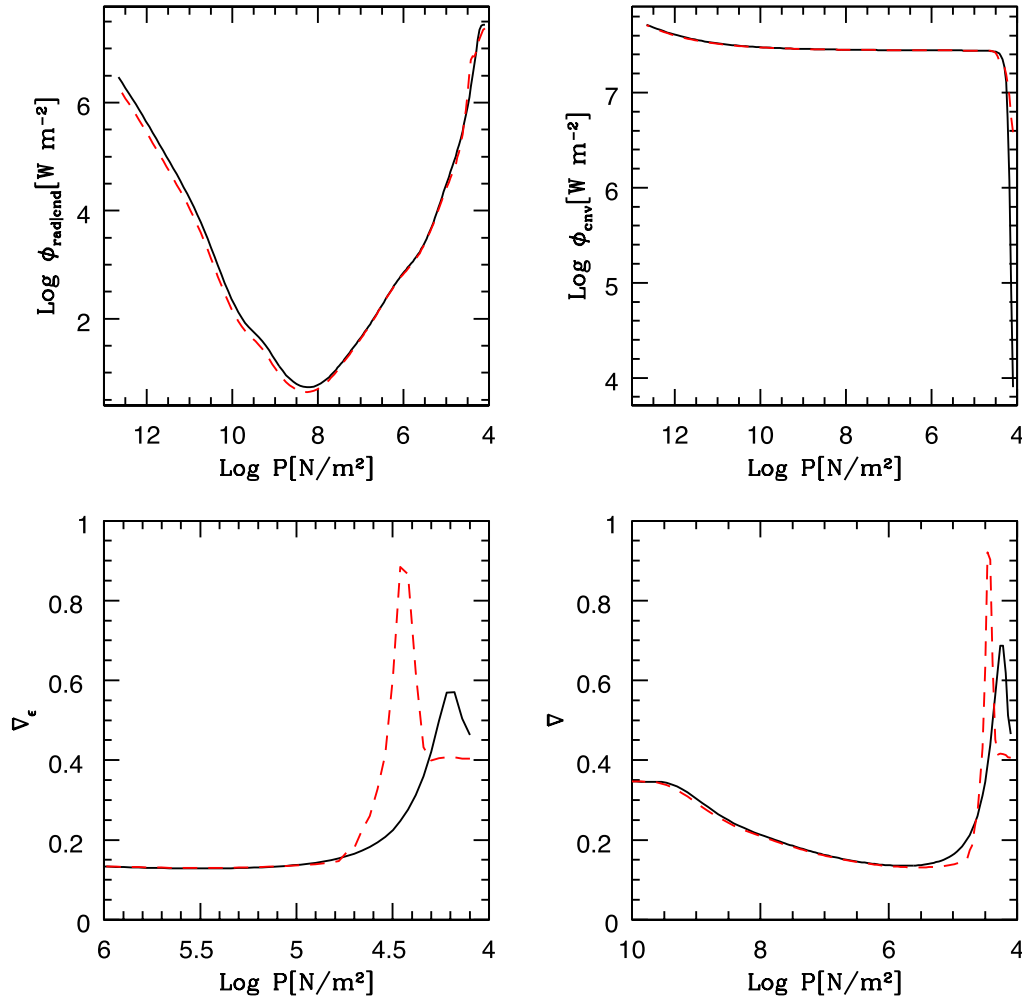
Figure 7. Structure of the outer layers of the Sun. Solar fluxes and temperature gradients profiles for the internal convective stratification of the star. The upper panels show the radiative flux $\varphi_{\mathrm{rad|cnd}}$ (left) and the convective flux φ_{cnv} (right). The bottom panels display the element gradient ∇_e (left) and the ambient gradient ∇ (right). The red dashed lines refer to SFC theory whereas the black solid lines to the ML theory.

The numerical code for the atmosphere models has been extracted from the classical Göttingen code developed by Hofmeister et al. (1964) and used and implemented by the Padova group for more than four decades. Over the years, this code has been developed to include semiconvection (e.g. Chiosi & Summa 1970), ballistic convective overshoot from the central core (Bressan, Chiosi & Bertelli 1981), envelope overshoot (Alongi et al. 1991), turbulent diffusive mixing and overshoot (Deng, Bressan & Chiosi 1996a,b; Salasnich, Bressan & Chiosi 1999), and finally the many revisions of the input physics and improvements described in Bertelli et al. (1994a, 1995, 2003, 2008), Bertelli & Nasi (2001). The version used here is the one by Bertelli et al. (1994b) in which we have replaced the ML theory with the SFC theory. The value of Λ_m adopted for the ML theory is taken from Bertelli et al. (2008) and provides calibrated models matching the properties of the Sun on the HRD. The adopted value is $\Lambda_m = 1.68$. The structure of the atmosphere models is according to the equations and physical input described in Sections 2, B1, and B2.

6.1 The outer layers of Sun-like stars: atmosphere models

We take the evolutionary track of 1 M$_\odot$ with chemical composition [X=0.71, Y=0.27, Z=0.02] calculated by Bertelli et al. (2008)

and isolate the model that fairly matches the position of the Sun on the HRD, i.e. $\log L/L_\odot$=0 and $\log T_{\mathrm{eff}}$=3.762. The atmosphere is shown in Fig. 7. In each panel we show the results for the standard ML theory (using $\Lambda = 1.68$ and the SFC theory. We display the radiative flux $\varphi_{\mathrm{rad|cnd}}$ (top left panel) and the convective flux φ_{conv} (top right panel), the logarithmic temperature gradient of the element ∇_e (bottom left panel) and of the medium ∇, (bottom right panel). The colour code indicates the underlying theory of convection, black for the ML theory and red for the new theory. It is soon evident that while the profiles of the fluxes are virtually identical with the two theories, the gradients ∇_e and ∇ are much different, a result already visible in Fig. 4. In both cases, the extent of convective zones is similar. By construction the position on the HRD is the same. For the sake of illustration we show in Fig. 8 the case of a 2.0 M$_\odot$ star with same chemical composition and in an advanced stage along the RGB, the luminosity is $\log L/L_\odot = 2.598$ and the effective temperature $\log T_{\mathrm{eff}} = 3.593$. The situation is much similar to the previous one. The new SFC theory yields the same path on the HRD as the calibrated MLT, however the greatest merit of former is that no ML parameter or calibration is required. The properties of convection are fully determined by the physics of the layer in which convection is at work. By taking the outer envelope of the model whose luminosity and effective temperature are those of the Sun
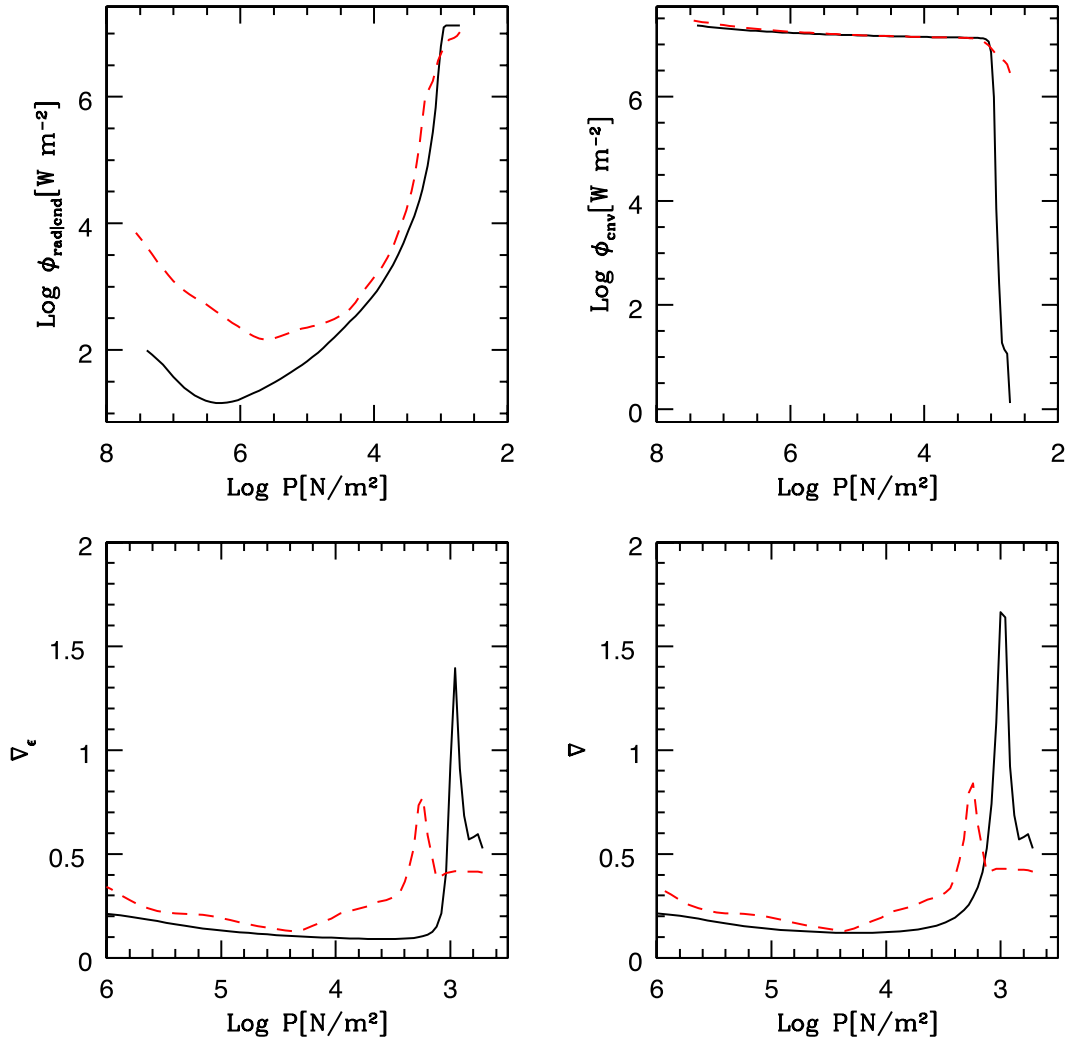
Figure 8. The same as in Fig. 7 but for the $2\,M_\odot$ in a late stage along the RGB, $\log L/L_\odot = 2.598$ and $\log T_{\rm eff} = 3.593$.

and looking at the stratification of the main variables (temperature, density pressure, radiative and convective fluxes, velocity and associated dimensions of convective elements, temperature gradient in presence of convection), it is soon evident that the ML theory is indeed a particular case in the more general solutions predicted by the SFC theory. As we go deeper into the atmospheres, the solutions for the ML theory and SFC theory tend to diverge. This is expected and it simply reflects the fact that these external solutions are not constrained to match the inner solution at the transition layer (typically $M/M_* \simeq 0.97$, where M and M_* are the mass at the layer r and total mass, respectively). Small differences among the two solutions tend to amplify as we go deeper inside. This is more evident in case of the $2.0\,M_\odot$ star along the RGB. This can be fixed only by considering complete stellar models. Hence a few preliminary exploratory stellar models will be presented below.

6.2 Preliminary, complete stellar models with the sfc theory

We have calculated a few test evolutionary sequences of complete stellar models for different initial mass and fixed chemical composition. The stellar models are followed from the main-sequence stage up to the end of the RGB or core helium exhaustion, as appropriate to the initial mass of the star.

Several important remarks are mandatory here before presenting the stellar models under consideration. First the SFC theory we have described is specifically designed to deal only with convection in the outer layers of the stars: it cannot be applied to deal with physical situations in which convective overshooting either from central cores and/or convective intermediate shells is taking place. However, we would like to mention that the formalism developed by Pasetto et al. (2014) derives the acceleration acquired by convective elements under the action of the buoyancy force in presence of the inertia of the displaced fluid and gravity. Therefore, it is best suited, with the necessary modification, to derive the motion of the convective elements beyond the formal limit set by the Schwarzschild condition, the penetration of these into the surrounding radiative regions, the dissipation of their kinetic energy and finally the redistribution of energy and physical properties of the layer interested by their motion, i.e. to describe convective overshooting. We are currently working on extending SFC theory to the convective overshooting (Pasetto et al., in preparation). Therefore, in order to calculate new stellar models with the SFC theory, we must use one of the prescriptions for convective overshooting from the core currently in literature. We adopt here the ballistic model of convective overshooting developed by Bressan et al. (1981) end since adopted by the Padova group. It is not the
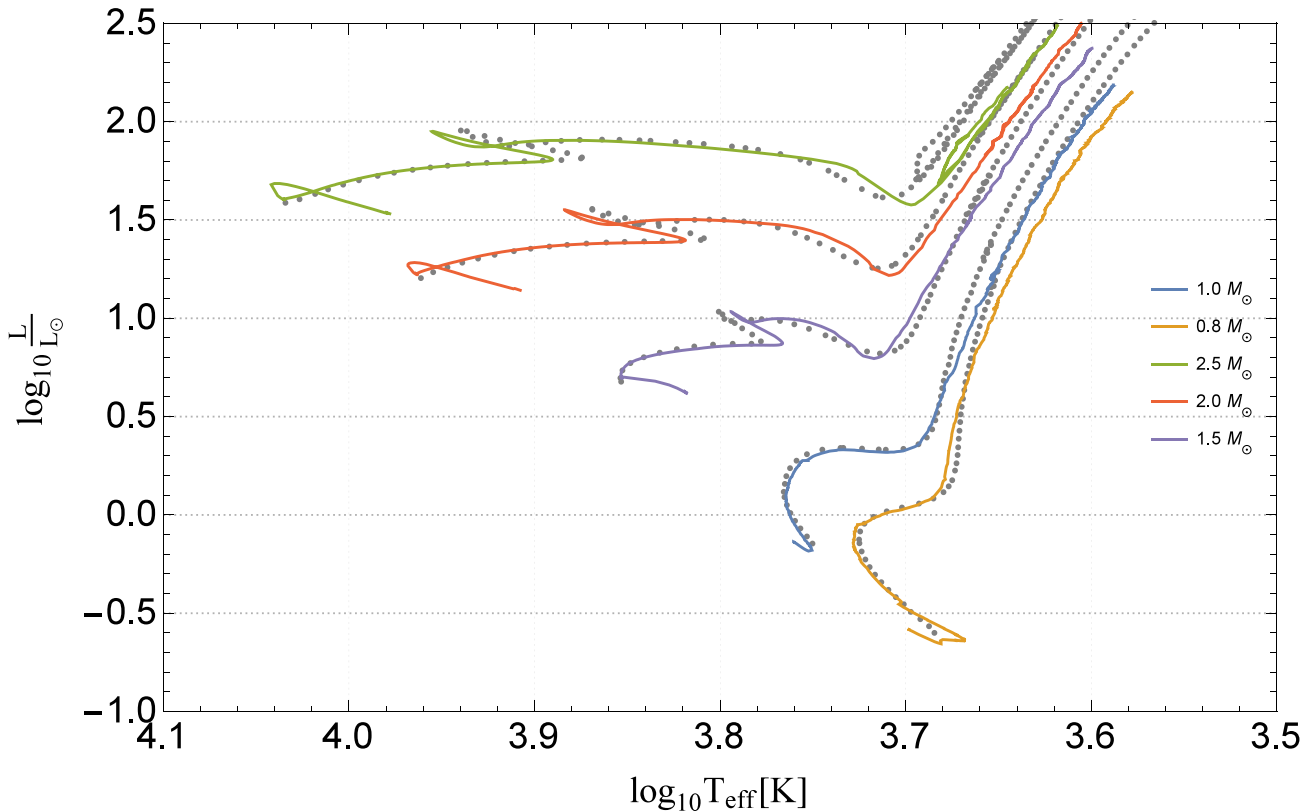
Figure 9. The HRD of the 0.8, 1.0, 1.5, 2.0, and 2.5 $M_\odot$ stars with initial chemical composition [$X = 0.703$, $Y = 0.280$, $Z = 0.017$] calculated from the main sequence to advanced evolutionary stages using both the classical ML theory (the dotted lines) and the SFC theory (solid lines of different colours). The 0.8, 1.0, 1.5 and 2.0 $M_\odot$ models are carried to a late stage of the RGB before core He-ignition (He-Flash), whereas the 2.5 $M_\odot$ is evolved up to very advanced stages of central He-burning ($Y_c \simeq 0.1$). The stellar models are calculated with the Padova code and input physics used by Bertelli et al. (1994b) and Bertelli et al. (2008), see also the text for more details. The models are meant to prove that the SFC theory with no ML parameter is very close to the classical ML theory with calibrated ML parameter ($\Lambda_m = 1.68$ in our case).

best solution but it is sufficient to obtain significant exploratory results.

The code considered in this models is the same from which we have taken all the routines to calculate the model atmospheres. All the input physics, i.e. opacities (radiative conductive and molecular), nuclear reaction rates, EoS, and the prescription for convective overshooting from the core are as described by Bertelli et al. (2008), to whom the reader should refer for all details. In particular, it is worth recalling that the treatment of core overshooting relies on Bressan et al. (1981) that stands on the ML theory (to derive the velocity of convective elements) and makes use of the ML parameter $\Lambda_c = 0.5$ for all masses $M_* \geq 1.5$ $M_\odot$, $\Lambda_c = 0$ for stars with mass $M_* \leq 1$ $M_\odot$, and finally $\Lambda_c = M_*/M_\odot - 1.0$ for stars in the interval $1.0 < M_*/M_\odot \leq 1.5$. Overshooting from the bottom of the convective envelope along the RGB follows from Alongi et al. (1991) with $\Lambda_e = 0.25$. Therefore, the interiors are calculated according to the classical prescription, whereas the outer layers are treated according to the SFC theory. This is an intermediate step towards the correct approach in which convective overshoot in the internal regions is treated in the framework of SFC theory.

We note that an obvious drawback of using the Bertelli et al. (1994b) code is that the input physics is somewhat out of date with respect to more recent versions of the same code, eg. Nasi et al. (2008), Bertelli et al. (2008, 2009), and finally the very recent revision of the whole code by Bressan et al. (2012), Chen et al. (2014)

and Tang et al. (2014). The choice of the Bertelli et al. (1994b) code is motivated by the large body of stellar models calculated with this and worldwide used. In any case, this satisfactorily permits the comparison of stellar models with the same code, input physics and both ML theory and SFC theory. Work is under way to calculate new grids of stellar models with SFC theory using an independent code with very modern input physics i.e. the Garching code named GARSTEC by Weiss & Schlattl (2008).

For the purposes of this exploratory investigation we present here five evolutionary sequences for stars of initial mass 0.8, 1.0, 1.5, 2.0, and 2.5 $M_\odot$ and chemical composition [$X = 0.703$, $Y = 0.280$, $Z = 0.017$] calculated from the main sequence to advanced evolutionary stages using both the classical ML theory ($\Lambda_m = 1.68$ in our case) and the SFC theory. The 0.8, 1.0, and 1.5 $M_\odot$ sequences are indicative of the old stars in Globular Clusters and very old Open Clusters, whereas the 2.0 and 2.5 $M_\odot$ sequences correspond to intermediate age Globular and Open clusters. The 2.0 $M_\odot$ is the last low mass star of the adopted chemical composition undergoing core He-Flash (Bertelli et al. 2008). The HR Diagram is shown in Fig. 9, where the grey dots indicate the sequences with the ML theory and the dotted lines of different colours show those with the SFC theory. The 0.8, 1.0, 1.5, and 2.0 $M_\odot$ models are carried to a late stage of the RGB before core He-ignition (He-Flash), whereas the 2.5 $M_\odot$ is evolved up to very advanced stages of central He-burning, $Y_c \simeq 0.1$ (no He-Flash has occurred). The corresponding models

with the classical ML theory (dotted paths) are taken from Bertelli et al. ([2008](#)).

In general the two sets of models are in close agreement. However looking at the results in some detail, the new tracks tends to have a slightly different inclination of the RGB. The SFC tracks are nearly identical to those of the ML theory at the bottom and progressively becomes redder towards the top, i.e. the RGBs of the low mass stars are less steep than those of the classical MLT models. Looking at the case of the 1 M$_\odot$ star, the MLT model are calculated with $\Lambda_m = 1.68$ upon calibration on the Sun and kept constant up to the end of the RGB and afterwards. The models with the SFC theory do not require the ML parameter but fully agree with the MLT ones during the core H-Burning phase but by the time they reach the RGB tip they would be in better agreement with MLT models with a smaller values of the ML parameter. The required decrease of Λ_m is difficult to quantify at the is stage of model calculations. However, it agrees with the analysis made by with Magic et al. ([2015](#)) of 3D radiative hydrodynamic simulations of convection in the envelopes of late-type stars in terms of the 1D classical ML theory. Using different calibrators and mapping the results a s function of gravity, effective and effective temperature Magic et al. ([2015](#)) find that at given gravity the ML parameter increases with decreasing effective temperature, the opposite at given effective temperature and decreasing gravity. There are also additional dependencies on metallicity and stellar mass that we leave aside here. Looking at the case of the Sun, passing from the main sequence to a late stage on the RGB, the ML is found to decrease by as much as about 10 per cent. Applying this to stellar models, a less steep RGB would result as shown by our model calculations with the SFC theory. Owing to the complexity of the new SFC theory with respect to the classical ML theory, the results are very promising. These preliminary model calculations show that that the SFC theory with no ML parameter is equivalent to the classical ML theory with calibrated ML. More work is necessary to establish a quantitative correspondence between the two theories of convection.

7 CONCLUSIONS AND FUTURE WORK

We have presented here the first results of the integration of stellar atmospheres and exploratory full stellar models to which the new convection theory developed by Pasetto et al. ([2014](#)) has been applied. To this aim, a mathematical and computational algorithm and a companion code have been developed to integrate the system of equations governing the convective and radiative fluxes, the temperature gradients of the medium and elements and finally, the typical velocity and dimensions of the radial and expansion/contraction motion of convective elements. In parallel we have also calculated the same quantities with the standard ML theory in which the ML parameter has been previously calibrated. All the results obtained with ML theory are recovered with the new theory but no scale parameters are adopted. We claim that the new theory is able to capture the essence of the convection in stellar interiors without a fine-tuned parameter inserted by hand.

The main achievement of the theory presented in this paper is not only to prove that satisfactory results can be achieved, as was already done by the ML theory, but more importantly to clarify that our understanding of the stellar structure is correct and fully determined by the underlying physics. Each star 'knows its own convection': i.e., where it is located, how much it extends and how much energy it is able to carry away. This is the meaning and the power of the self-consistent results we have just presented. Finally, the theoretical picture we have developed has a predictive power

that merely descriptive analyses of numerical simulations still miss. In other words, successful numerical experiments of laboratory hydrodynamics with millions of degrees of freedom do not imply a complete understanding of the phenomenon under investigation. An emblematic example of this is offered by the impressive simulations by Arnett et al. ([2015](#)). However, even in this case the closure of the basic equations involved in their hydrodynamic simulations is not possible. This has been instead achieved by the much simpler and straightforward formulation of the same problem by Pasetto et al. ([2014](#)). Based on these preliminary results we are confident that this is the right path to follow. However, before moving towards more complicated physical situations such as convective overshoot and semiconvection and extending our theory to deal with these phenomena (Pasetto et al., in preparation), it is necessary to check the overall consistency of the new theory by calculating stellar models over all possible evolutionary phases according to the mass of the star, to extend the calculations to wider ranges of initial masses (namely to massive stars where mass loss by stellar winds is important all over their evolutionary history and the very low mass ones where convection is becoming more and more important), and finally to consider other initial chemical compositions. Work is in progress to this aim (Pasetto et al., in preparation).

Finally, a numerical code for the solution of the polynomial (12) or (10) both in ξ_e and $|v|$ is available upon request to the first author.

REFERENCES

Alongi M., Bertelli G., Bressan A., Chiosi C., 1991, A&A, 244, 95
Arnett W. D., Meakin C., Viallet M., Campbell S. W., Lattanzio J., Moćak M., 2015, ApJ, 809, 30
Augustson K. C., Brown B. P., Brun A. S., Miesch M. S., Toomre J., 2012, ApJ, 756, 169
Baker N., Kippenhahn R., 1962, Z. Astrophys., 54, 114
Balmforth N. J., 1992, MNRAS, 255, 603
Batchelor G. K., 2000, in Batchelor G. K., ed., An Introduction to Fluid Dynamics. Cambridge Univ. Press, Cambridge, p. 615
Bazán G., Arnett D., 1998, ApJ, 496, 316
Bertelli G., Nasi E., 2001, AJ, 121, 1013
Bertelli G., Bressan A., Chiosi C., Ng Y. K., Ortolani S., 1994a, Mem. Soc. Astron. Ital., 65, 689
Bertelli G., Bressan A., Chiosi C., Fagotto F., Nasi E., 1994b, A&AS, 106, 275
Bertelli G., Bressan A., Chiosi C., Ng Y. K., Ortolani S., 1995, A&A, 301, 381
Bertelli G., Nasi E., Girardi L., Chiosi C., Zoccali M., Gallart C., 2003, AJ, 125, 770
Bertelli G., Girardi L., Marigo P., Nasi E., 2008, A&A, 484, 815
Bertelli G., Nasi E., Girardi L., Marigo P., 2009, A&A, 508, 355
Biermann L., 1951, Z. Astrophys., 28, 304
Biskamp D., 1993, Nonlinear Magnetohydrodynamics. Cambridge Univ. Press, Cambridge, p. 378

Böhm-Vitense E., 1958, Z. Astrophys., 46, 108

Bressan A. G., Chiosi C., Bertelli G., 1981, A&A, 102, 25

Bressan A., Marigo P., Girardi L., Salasnich B., Dal Cero C., Rubele S., Nanni A., 2012, MNRAS, 427, 127

Brown T. M., Gilliland R. L., 1994, ARA&A, 32, 37

Brown B. P., Browning M. K., Brun A. S., Miesch M. S., Toomre J., 2008, ApJ, 689, 1354

Brun A. S., Toomre J., 2002, ApJ, 570, 865

Brun A. S., Miesch M. S., Toomre J., 2011, ApJ, 742, 79

Canuto V. M., Mazzitelli I., 1991, ApJ, 370, 295

Canuto C., Hussaini M. Y., Quarteroni A., Zang T. A., 2006, Spectral Methods. Springer-Verlag, Berlin Heidelberg

Chandrasekhar S., 1960, Radiative Transfer. Dover Publications Inc., Mineola, New York

Chaplin W. J., 2013, in Jain K., Tripathy S. C., Hill F., Leibacher J. W., Pevtsov A. A., eds, ASP Conf. Ser. Vol. 478, Fifty Years of Seismology of the Sun and Stars. p. 101

Chaplin W. J., Miglio A., 2013, ARA&A, 51, 353

Chen Y., Girardi L., Bressan A., Marigo P., Barbieri M., Kong X., 2014, MNRAS, 444, 2525

Chiavassa A., Bigot L., Thévenin F., Collet R., Jasniewicz G., Magic Z., Asplund M., 2011, J. Phys. Conf. Ser., 328, 012012

Chiosi C., Summa C., 1970, Ap&SS, 8, 478

Christensen-Dalsgaard J., 2002, Rev. Mod. Phys., 74, 1073

Collet R., Magic Z., Asplund M., 2011, J. Phys. Conf. Ser., 328, 012003

Cox J. P., Giuli R. T., 1968, Principles of Stellar Structure - Vol.1: Physical Principles; Vol.2: Applications to Stars.

Cubarsi R., 2010, A&A, 522, A30

Deng L., Bressan A., Chiosi C., 1996a, A&A, 313, 145

Deng L., Bressan A., Chiosi C., 1996b, A&A, 313, 159

Glatzmaier G. A., 2013, Introduction to Modelling Convection in Planets and Stars.

Grossman S. A., 1996, MNRAS, 279, 305

Hofmeister E., Kippenhahn R., Weigert A., 1964, Z. Astrophys., 59, 215

Hughes D. W., Rosner R., Weiss N. O., 2012, The Solar Tachocline.

Ishihara T., Kaneda Y., Yokokawa M., Itakura K., Uno A., 2007, J. Fluid Mech., 592, 335

Ishihara T., Gotoh T., Kaneda Y., 2009, Annu. Rev. Fluid Mech., 41, 165

Jenkins M., Traub J., 1970, Numer. Math., 14, 252

Jimenez J., Kawahara G., 2014, in Davidson P. A., Kaneda Y., Sreenivasan K. R., eds, Dynamics of wall-bounded turbulence. Cambridge Univ. Press, Cambridge, UK

Kenada Y., Morishita K., 2014, in Davidson P. A., Kaneda Y., Sreenivasan K. R., eds, Small-Scale Statistics and Structure of Turbulence - in the Light of High Resolution Direct Numerical Simulation. Cambridge Univ. Press, Cambridge, UK

King B. R., 2008, Beyond the Quartic Equation, Modern Birkhäuser Classics, 2nd edn. 2009. Athens, GA, USA

Kippenhahn R., Weigert A., 1994, Stellar Structure and Evolution.

Kippenhahn R., Weigert A., Weiss A., 2012, Stellar Structure and Evolution.

Kueker M., Ruediger G., Kitchatinov L. L., 1993, A&A, 279, L1

Landau L. D., Lifshitz E. M., 1959, Fluid Mechanics, Pergamon Press, UK

Landau L. D., Lifshitz E. M., 1969, Mechanics, Pergamon Press, UK

Ludwig H.-G., Jordan S., Steffen M., 1994, A&A, 284, 105

Ludwig H.-G., Freytag B., Steffen M., 1999, A&A, 346, 111

Lydon T. J., Fox P. A., Sofia S., 1992, ApJ, 397, 701

Maeder A., 2009, Physics, Formation and Evolution of Rotating Stars. Springer-Verlag, Berlin

Magic Z., Collet R., Asplund M., Trampedach R., Hayek W., Chiavassa A., Stein R. F., Nordlund Å., 2013, A&A, 557, A26

Magic Z., Weiss A., Asplund M., 2015, A&A, 573, A89

Meakin C. A., Arnett D., 2007, ApJ, 667, 448

Miesch M. S., Brun A. S., De Rosa M. L., Toomre J., 2008, ApJ, 673, 557

Mihalas D. M., 1982, Stellar Atmospheres [translated from the English edn. Mir, Moskva. Part I, p. 352, Part II, p. 424. In Russian]

Nasi E., Bertelli G., Girardi L., Marigo P., 2008, Mem. Soc. Astron. Ital., 79, 738

Orszag S. A., 1971, J. Fluid Mech., 49, 75

Orszag S. A., Patterson G. S., 1972, Phys. Rev. Lett., 28, 76

Ottino J. M., 1989, The Kinematics of Mixing, Cambridge texts in applied mathematics. Cambridge Univ. Press, Cambridge

Pasetto S., Chiosi C., 2009, A&A, 499, 385

Pasetto S., Bertelli G., Grebel E. K., Chiosi C., Fujita Y., 2012, A&A, 542, A17

Pasetto S., Chiosi C., Cropper M., Grebel E. K., 2014, MNRAS, 445, 3592

Pinheiro F. J. G., Fernandes J., 2013, MNRAS, 433, 2893

Prandtl L., 1925, Math. Meth., 5, 136

Salaris M., Cassisi S., 2015, A&A, 577, A60

Salasnich B., Bressan A., Chiosi C., 1999, A&A, 342, 131

Somov B. V., 2006, Plasma Astrophysics, Part I: Fundamentals and Practice. Springer-Verlag, Berlin

Tang J., Bressan A., Rosenfield P., Slemer A., Marigo P., Girardi L., Bianchi L., 2014, MNRAS, 445, 4287

Tuteja G. S., Khattar D., Chakraborty B. B., Bansal S., 2010, Int. J. Contemp. Math. Sciences, 5, 1065

Rhodes, E. J., JrUlrich R. K., 1977, ApJ, 218, 521

Weiss A., Schlattl H., 2008, Ap&SS, 316, 99

APPENDIX A: THE EXTERNAL LAYERS: BASIC EQUATIONS AND INPUT PHYSICS

In these appendices, we provide the precise disposition of the equations we have used in this paper, with the aim of enhancing the ease with which our results can be replicated and checked.

We start with the treatment we have used for the photosphere.

A1 The photosphere

Given the total mass M_* and the chemical composition $[X, Y, Z]$ (following standard notation, X represents the H concentration, Y the He and Z the remaining elements so that $X + Y + Z = 1$ identically holds), and adopting the spherical symmetry, and a system of polar coordinates $x = \{r, \theta, \phi\}$ centred on the barycentre of a star, the boundary conditions at the surface of a star are

$$r = r_* \qquad T_{\text{sup}} = T_{\text{ph}} \qquad \rho_{\text{sup}} = \rho_{\text{ph}}. \qquad (A1)$$

Determining T_{ph} and ρ_{ph} (or P_{ph}) is not simple, requiring a detailed treatment of the external layers of a star. The photosphere, which corresponds to the surface of a star, is defined as the most external layer from which the radiation coming from inside is eventually radiated away and above which the Local Thermodynamic Equilibrium can no longer be applied. It is the last layer at which the radiation is nearly identical to that of a blackbody at the temperature T. This layer is also used to define the effective temperature T_{eff} implicitly as

$$L = 4\pi r_*^2 \sigma T_{\text{eff}}^4. \qquad (A2)$$

The photosphere is also the layer at which the matter is no longer transparent to radiation. We make use of the concept of optical depth at the photon frequency ν, κ_ν, the Eddington approximation (i.e. independence of the specific frequency ν) for the radiative transfer equation and the grey body approximation. The momentum flux equation for a photon fluid reads

$$\frac{\partial \varphi}{\partial t} + \langle \nabla_x, \boldsymbol{P}_{\nu \text{rad}} \rangle = -\rho \kappa_\nu \varphi, \qquad (A3)$$

where φ is the radiative flux of photons and $\boldsymbol{P}_{\nu \text{rad}}$ is the pressure radiation tensor for photons of frequency ν and $\langle \bullet, \bullet \rangle$ denotes the inner product. Eddington introduced the function K_ν which is widely used in the literature and is related to the outward component of the monochromatic pressure tensor $P_{\text{rad}, \nu}$ of frequency ν as $P_{\text{rad}, \nu} = 4\pi K_\nu$ together with two functions: H_ν (the Eddington

flux) and F_ν related by $P_{\mathrm{rad},\,\nu} = 4\pi H_\nu = \pi F_\nu$.[4] Making use of the grey-body approximation and this notation, equation (A3) reads

$$\frac{\mathrm{d}K}{\mathrm{d}\tau} = \frac{F}{4}. \tag{A4}$$

Because we assumed radiative equilibrium, we can integrate the above equation to obtain the mean intensity $I = \frac{1}{4\pi} \oint I \,\mathrm{d}\Omega$ over the solid angle $\mathrm{d}\Omega$ as

$$I = \frac{3}{4} F\left(\tau + Q\right), \tag{A5}$$

where the Eddington condition $I = 3K$ has been employed on equation (A4) and Q is the integration constant. For a linear intensity relation, $I_\nu = a\mu + b$ with $\mu = \cos\theta$ cosine director outwards from the star pointing to us, we can fit the Sun limb darkening with $\frac{a}{b} \cong \frac{3}{2}$ and determine the constant Q (normalized to the Sun) as $Q \cong \frac{2}{3}$. Finally, if we assume that in the stellar layer considered the mean-free-path of a photon is much smaller than the characteristic scalelength where the temperature changes, $\lambda_\nu = \frac{1}{\rho\kappa} \ll h_T$, the diffusion-approximation applies ($I \cong \frac{a}{4\pi} T^4$) and with the definition of effective temperature above, we obtain:

$$T^4 = \frac{3}{4}\left(\tau + \frac{2}{3}\right) T_{\mathrm{eff}}^4. \tag{A6}$$

Therefore, the photosphere is the layer whereby $\tau = 2/3$. A more rigorous solution by Chandrasekhar (1960) (see also Mihalas 1982, p. 62) sees the factor $\frac{2}{3}$ in the previous equation substituted by $q(\tau) \in \,]0.577, 0.710[$. This relation yields the dependence of the temperature on the optical depth in the region $\tau = 0$ ($\rho = 0$) to $\tau = 2/3$ in the grey atmosphere approximation.

Finally, the pressure at the photosphere is given by the hydrostatic equilibrium condition as a function of τ,

$$P_{\mathrm{ph}} = \frac{Gm}{r^2} \int_0^{\tau_{\mathrm{ph}}} \frac{1}{\kappa}\mathrm{d}\tau, \tag{A7}$$

where $P_{\mathrm{ph}} = 0$ at $\tau = 0$ and radiation pressure is neglected and G is the gravitational constant. The opacity κ is a function of position, $\kappa = \kappa(r)$, and therefore the state variables P, T, ρ, and chemical composition μ. However, to a first approximation κ can be considered constant. It follows from this that

$$P_{\mathrm{ph}} = \frac{2}{3} \frac{1}{\kappa_{\mathrm{ph}}} \frac{Gm}{r^2} \tag{A8}$$

Note that the effect of radiation pressure the can be absorbed by recasting in the above equation the gravity as $g_{\mathrm{eff}} = g - \frac{\kappa \sigma T_{\mathrm{eff}}^4}{c}$ with $g = \frac{GM}{r^2}$. The relationships for T_{ph} and P_{ph} define the natural boundary conditions for the system of equations describing a stellar structure. To conclude, temperature, pressure and density in the regions above the photosphere are expressed as functions of the optical depth τ, whereas below the photosphere to be determined they require the complete set of stellar structure equations.

A2 The atmosphere

In absence of rotation, magnetic fields and in hydrostatic equilibrium, the structure of a star is defined by the following equations:

(i) The mass conservation

$$\frac{\mathrm{d}M}{\mathrm{d}r} = 4\pi r^2 \rho, \tag{A9}$$

where $M = M(r)$ is the mass inside the sphere of radius r.

(ii) The gravitational potential $\Phi_{\mathbf{g}}$ satisfying the Poisson relation

$$\frac{\mathrm{d}\Phi_{\mathbf{g}}}{\mathrm{d}r} = 4\pi g\rho. \tag{A10}$$

(iii) The condition of mechanical equilibrium for a fluid at rest (Euler equation):

$$\frac{\mathrm{d}P}{\mathrm{d}r} = -\rho\frac{GM}{r^2}, \tag{A11}$$

with G is the gravitational constant.

(iv) The equation for the energy conservation

$$\frac{\mathrm{d}L}{\mathrm{d}r} = 4\pi r^2 \rho(\varepsilon_N - \varepsilon_\nu + \varepsilon_g), \tag{A12}$$

where $\varepsilon_N, \varepsilon_\nu$ and ε_g are the nuclear, neutrino losses, and gravitational sources, respectively.

(v) Finally, the equation for energy transfer, which can be expressed as follows

$$\frac{\mathrm{d}\ln T}{\mathrm{d}\ln P} = \nabla, \tag{A13}$$

where ∇ depends on the dominating physical mechanism for energy transport: $\nabla_{\mathrm{rad/cnd}}$ for radiation plus conduction, ∇_{cnv} for convection (typically in stellar atmospheres), and simply ∇_{ad} in presence of adiabatic convection (typically in deep stellar interiors).

In the atmosphere, first it is more convenient to use the pressure P instead of the radius r as the independent variable, and second all the three energy sources ϵ_n, ϵ_g, and ϵ_ν can be assumed to be zero so that the luminosity is a constant $L(M) = L = \mathrm{const}$. Consequently equation (A12) is no longer needed and equations (A9), (A11), (A13) read:

$$\begin{cases} \frac{\mathrm{d}\ln M}{\mathrm{d}\ln P} = -\frac{4\pi r^4 P}{GM^2} \\[2mm] \frac{\mathrm{d}\ln r}{\mathrm{d}\ln P} = -\frac{rP}{G\rho M} \\[2mm] \frac{\mathrm{d}\ln T}{\mathrm{d}\ln P} = \nabla, \end{cases} \tag{A14}$$

with $L(P) = L = \mathrm{constant}$. respectively.

These equations must be complemented by the EoS in the atmosphere, $P = P(\rho, T, \mu)$ with μ the molecular weight of the chemical mixture (inclusive of ionization), the opacity $\kappa(\rho, T, \mu)$, and the expressions for ∇ that depend on the transport mechanism at work. If $\nabla_{\mathrm{rad}} < \nabla_{\mathrm{ad}}$, the energy flows by radiative transport and the temperature gradient of the medium is

$$\nabla = \nabla_{\mathrm{rad}} = \frac{3}{16\pi acG} \frac{\kappa L P}{M T^4}, \tag{A15}$$

with a density-radiation constant and c speed of light. If $\nabla_{\mathrm{rad}} \geq \nabla_{\mathrm{ad}}$ convection sets in, and the energy flux is carried by radiation and convection. we indicate with $\varphi, \varphi_{\mathrm{cnv}}$ and $\varphi_{\mathrm{rad|cnd}}$ the total energy flux, the convective flux, and the radiative plus conductive (if needed) energy flux lumped together.[5] Among the three fluxes the obvious

---

[4] These functions can be proved to be simply statistical moments of the intensity weighted by $\cos\theta$ and $\cos^2\theta$ related to the radiative flux and the radiative pressure in any direction θ pointing outside the star to the observer.

[5] Conduction has an important role in the degenerate cores of red giants and advanced stages of intermediate-mass and massive stars, and dominates in the isothermal cores of white dwarfs and neutron stars. The conductive flux can be expressed by the same relation for the radiative flux provided the opacity is suitably redefined. In the external layers of a normal star

equation $\varphi = \varphi_{cnv} + \varphi_{rad|cnd}$ applies. In this region four temperature gradients are at work: the gradient of convective elements ∇_e, the gradient of the medium in presence of convection ∇_{cnv}, the adiabatic gradient ∇_{ad}, and a fictitious gradient still named ∇_{rad} as if all the energy flux were carried by radiation. While the flux carried by radiation is easily known, the flux carried by convection requires a suitable theory, to specify ∇ and ∇_e. The above system of equations (A14) together with those describing the convective transport represent the environment of the stellar atmosphere in which super-adiabatic convection is at work either according to the ML theory or the new SFC theory that will be shortly summarized in Appendix B.

To complete the physical description of the stellar medium, we need to present here thermodynamic quantities that are used to derive temperature gradients and the convective flux in presence of ionization and radiation pressure.

A3 Ionization and thermodynamics of an ionizing gas

To proceed with the calculation of ∇_e and ∇ required by the systems of equations (B1) for ML theory or (1) for the SFC theory we need ∇_{ad} and c_P for a gas made of a number elemental species in various degrees of ionization and in presence of radiation pressure. Despite several formulations of this equation exist in literature (e.g. Baker & Kippenhahn 1962; Hofmeister et al. 1964; Cox & Giuli 1968; Kippenhahn & Weigert 1994; Kippenhahn et al. 2012), we present here the basic equations adopted in this paper. They are taken from Baker & Kippenhahn (1962) however adapted to our notation and strictly limited to those used in our code.

A3.1 Ionization

Consider a mixture of atoms of type $i = 1, ..., N$, each of which with $n_{e,i}$ electrons and $n_{e,i} + 1$ stages of ionization indicated by $r = 0, ..., n_{e,i}$ (we neglect here the case of atoms in a give stage of ionization but different state of excitation), the fraction of atoms of type i in the ith stage of ionization (i.e. that have lost i electrons) is x_i^r. The total fraction y_i^j of atoms of type i which are in ionization stages higher than ith is $y_i^r = \sum_{s=r+1}^{n_{e,i}} x_i^s$. Let us indicate the relative number of atoms of type i as $\nu_i = n_i/n$ with n total atoms of N types. The total fraction f_e of free electrons is then:

$$f_e = \sum_{i=1}^{N} \nu_i \sum_{r=0}^{n_{e,i}} r x_i^r = \sum_{i=1}^{N} \sum_{r=0}^{n_{e,i}-1} \nu_i y_i^r . \tag{A16}$$

We introduce the function

$$K_i^r \equiv \frac{u_{r+1}}{u} \frac{2}{P_{gas}} \frac{(2\pi m_e)^{3/2} (k_B T)^{5/2}}{h^3} e^{-\frac{\chi_i^r}{k_B T}}, \tag{A17}$$

for $r = 0, 1, ...Z_{i-1}$, where χ_i^r is the rth ionization potential of atom i, u the statistical weight of the state r, k_B the Boltzmann constant and h the Plank constant. Then, to derive the degree of ionization we need to solve the system of $\sum_{i=1}^{N}(n_{e,i} - 1)$ Saha's equations together with the N equations $\sum_{r=0}^{n_{e,i}} x_i^r = 1$ for the $\sum_{i-1}^{N} n_{e,i}$ quantities X_i^r:

$$\begin{cases} \frac{x_i^{r+1}}{x_i^r} \frac{f_e}{f_e+1} = K_i^r \\ \sum_{r=0}^{n_{e,i}} x_i^r = 1, \end{cases} \tag{A18}$$

conduction in practice has no role and the above notation is superfluous. However in view of the future extension of the SFC theory to internal convection and/overshooting, we keep also here this more general notation.

that can be solved numerically. In most cases, however, the ionization potentials χ_i^r differ sufficiently from each other so that only one ionization is taking place at any time. Therefore for a given $i = k$ only x_k^s and x_k^{s+1} are different from zero. The condition ($\sum_{r=0}^{n_{e,i}} x_i^r = 1$ can then be approximated by $x_i^s + x_i^{s+1} = 1$ and accordingly $y_k^r = 0$ for $r > s$, $y_k^s = x_k^{s+1}$, and $y_k^r = 1$ for $r < s$, and the Saha's equation becomes a quadratic expression:

$$\frac{y_k^s}{1 - y_k^s} \frac{A_k^s + \nu_k Y_k^s}{1 + A_k^s + \nu_k y_k^s} = K_k^s, \tag{A19}$$

with the aid of the auxiliary quantity

$$A_k^s \equiv \sum_{i \neq k}^{N} \sum_{r=0}^{n_{e,i}-1} \nu_i y_i^r + \nu_k \sum_{r \neq s}^{n_{e,i}-1} y_k^r, \tag{A20}$$

that has a fully algebraic solution.

A3.2 Thermodynamics

The derivation of ∇_{ad} and c_P accounting for the effect of ionization is as follows. In equation (A16) and (A20) we absorb the indexes over the atoms and ionization, i.e. we write simply $f_e = \sum_{i=1}^{N} \nu_i y_i$ and $A_k \equiv \sum_{i \neq k}^{N} \nu_i y_i$. Then, for any stellar layer the specific heat c_p is

$$c_P = \frac{\Re}{\mu_0} \left(\frac{5}{2} + \frac{4(1-\beta)(4+\beta)}{\beta^2} \right) (1 + f_e) + \sum_i \frac{\nu_i}{G_i} F_i^2, \tag{A21}$$

where the auxiliary functions F_i and G_i are

$$\begin{aligned} F_i &\equiv \frac{5}{2} + \frac{4(1-\beta)}{\beta} + \frac{\chi_i}{k_B T} \\ G_i &\equiv \frac{1}{y_i(1-y_i)} + \frac{\nu_i}{f_e(1+f_e)}, \end{aligned} \tag{A22}$$

where $\quad 1 - \beta = \frac{aT^4}{3P}, \quad \mu = \frac{\mu_0}{1+f_e}, \quad \delta = -\left(\frac{\partial \ln \rho}{\partial \ln T}\right)_P,$ and $\alpha = -\left(\frac{\partial \ln \rho}{\partial \ln P}\right)_T$ have been used. Finally, under the same hypotheses, the adiabatic gradient is

$$\nabla_{ad} = \frac{\left(1 + \frac{(1-\beta)(4+\beta)}{\beta^2}\right)(1 + f_e) + \frac{1}{\beta} \sum_i \frac{\nu_i}{G_i} F_i}{\left(\frac{5}{2} + \frac{4(1-\beta)(4+\beta)}{\beta^2}\right)(1 + f_e) + \sum_i \frac{\nu_i}{G_i} F_i^2}. \tag{A23}$$

where ∇_{ad} is 0.4 for a perfect neutral gas with no radiation, tends to 0.25 for a fully ionized gas in presence of radiation, and may further decrease to about 0.12 in presence of ionization as in the case of external layers. Finally, the generalized adiabatic exponent Γ_1 (that is needed to calculate the sound velocity) is

$$\Gamma_1 = \left(2\beta(3\beta(\beta + 8) - 32)(f_e + 1)G_i - 4\beta^3 F_i^2 \nu_i \right)$$
$$\times (\nu_i (\beta (2F_i + 3) - 8) ((8 - \beta (2F_i + 3)) - 8\beta) \tag{A24}$$
$$+ 6\beta (7\beta - 8) (f_e + 1) G_i + \beta \nu_i (\beta (4F_i + 39) - 64))^{-1}.$$

All the model atmospheres used in this study are calculated including radiation pressure and ionization of light elements and the effect of these on all thermodynamical quantities in use. For more details the reader should refer to the original sources (Baker & Kippenhahn 1962; Hofmeister et al. 1964; Cox & Giuli 1968; Kippenhahn & Weigert 1994; Kippenhahn et al. 2012).

APPENDIX B: THE ML AND SFC THEORIES OF CONVECTION

The above equation of stellar structure in the atmosphere require a suitable theory of convection. In this appendix first we summarize the version of the classical ML theory we have adopted and then we shortly review the new SFC theory of Pasetto et al. (2014) In what follows we will omit the proofs of the results to focus attention on the resolution techniques of the equations presented.

B1 ML theory: a summary

The equations for the energy flux transport of the ML theory are available from the literature in several forms (equivalent in content). They are

$$
\begin{cases}
\varphi_{\mathrm{rad|cnd}} = \frac{4ac}{3} \frac{T^4}{\kappa h_p \rho} \nabla \\[2mm]
\varphi_{\mathrm{rad|cnd}} + \varphi_{\mathrm{cnv}} = \frac{4ac}{3} \frac{T^4}{\kappa h_p \rho} \nabla_{\mathrm{rad}} \\[2mm]
v^2 = g\delta (\nabla - \nabla_e) \frac{l_m^2}{8 h_p} \\[2mm]
\varphi_{\mathrm{cnv}} = \rho c_P T \sqrt{g\delta} \frac{l_m^2}{4\sqrt{2}} h_p^{-3/2} (\nabla - \nabla_e)^{3/2} \\[2mm]
\frac{\nabla_e - \nabla_{\mathrm{ad}}}{\nabla - \nabla_e} = \frac{6ac T^3}{\kappa \rho^2 c_P l_m v},
\end{cases}
\tag{B1}
$$

where h_p is the scaleheight of the pressure stratification of the star, v the average velocity of the convective element, and all other symbols have their usual meaning. In particular we recall that l_m is the mean dimension and mean free path of the convective elements before dissolving and releasing their energy excess to the surrounding medium. It is customarily expressed as $l_m = \Lambda_m h_p$, where Λ_m is the ML parameter. The derivation and solution of this system of equations can be found in any classical textbook of stellar structure (e.g. Kippenhahn & Weigert 1994; Hofmeister et al. 1964; Kippenhahn et al. 2012). In the literature, there are several versions of the ML theory (see Pasetto et al. 2014, and references) but in this paper we prefer to follow the one presented by Hofmeister et al. (1964) and adopted by the Padova group in their stellar evolution code to calculate the structure of the most external layers of a star (see Bertelli et al. 2008, and references).

The set of equations (B1) can be lumped together in a dimensionless equation among the three gradients ∇ (of the medium in presence of convection), ∇_{rad}, and ∇_{ad}. Introducing the quantity

$$
V \equiv \frac{3ac T^3}{c_P \rho^2 \kappa l_m^2} \sqrt{\frac{8 h_p}{g\delta}}
\tag{B2}
$$

$$
W \equiv \nabla_{\mathrm{rad}} - \nabla_{\mathrm{ad}},
$$

we may derive from system equation (B1) the dimensionless equation

$$
(\xi - V)^3 + \frac{8}{9} V \left(\xi^2 - V^2 - W \right) = 0,
\tag{B3}
$$

where ξ is the positive root of $\xi^2 = \nabla - \nabla_{\mathrm{ad}} + V^2$. The solution of equation (B3) is algebraic. Writing equation (B3) in standard form

$$
\xi^3 - \frac{17 U^3}{9} - \frac{19 U}{9} \xi^2 + 3 U^2 \xi - \frac{8 U W}{9} = 0,
\tag{B4}
$$

and using the Tschirnhaus transformation, $\xi = \eta + \frac{19 U}{9}$, we get

$$
\eta^3 + \frac{368}{243} U^2 \eta - \frac{9344}{19683} U^3 - \frac{8}{9} U W = 0.
\tag{B5}
$$

Writing this equation in the compact form $\eta^3 + py + q = 0$, the associated discriminant is $\Delta = -4p^3 - 27 q^2 < 0$. Hence, we expect the solutions of equation (B3) to have only one real root given by

$$
\eta = \sqrt[3]{\frac{1}{2} \left(-q + \sqrt{q^2 + \frac{4}{27} p^3} \right)} + \sqrt[3]{\frac{1}{2} \left(-q - \sqrt{q^2 + \frac{4}{27} p^3} \right)}
\tag{B6}
$$

with $p = \frac{368}{243} V^2$ and $q = -\frac{9344}{19683} V^3 - \frac{8}{9} V W$. Inverting the Tschirnhaus transformation we obtain the final solution. Once ∇ is known, one may derive ∇_e from the relation $\nabla_e - \nabla_{\mathrm{ad}} = 2V \sqrt{\nabla - \nabla_e}$, so that the four gradients and the fluxes φ_{rad} and φ_{cnv} are determined, and the whole problem is solved. Despite this apparent simplicity, in the literature there are several different expressions for the coefficient of the cubic equation (Cox & Giuli 1968; Maeder 2009; Kippenhahn et al. 2012, e.g.) or even for the equation system equation (B1). We will keep the solution obtained from the above equations.

B2 The new theory of stellar convection

The drawback of the ML theory is the ML parameter that cannot be determined in the framework of the ML theory itself. Vice versa the theory proposed by Pasetto et al. (2014) describes the motion of convective elements taking into account that in addition to the upward /downward motion due to the buoyancy force they also expand/contract while moving so that they are subjected to other effects. By doing this, new equations are found which together with those based on the energy conservation lead to a self-consistent description of the motions of convective elements without introducing arbitrary free parameters. As expected, the physics of the medium itself determines all the properties of convection at each unstable layer of a star.

The key idea of the new theory of stellar convection by Pasetto et al. (2014) is simple. Considering a rising convective element, in a 1D model of a star, because of the spherical symmetry, the motion occurs along the radial direction, while at the same time the element increases its dimension. The opposite happens for an element sinking into the medium: we have radial motion and shrinkage. The upward (downward) motion and expansion (shrinkage) of the element are intimately related (indeed the element rises because it expands and sinks because it shrinks). We remind the reader that in the classical ML theory only the radial motion is explicitly considered whereas expansion and shrinkage although implicitly present are not taken into account. We emphasize that the presence of the ML parameter simply mirrors the incomplete description of the motion of convective elements that is limited to the radial direction. Therefore the natural trail to follow to develop an alternative scale-free theory of convection is to look at the expansion/contraction, the radial motion being physically connected. The goal can be easily achieved if instead of using the natural reference frame S_0 centred on a star's centre (inertial system), we make use of a frame of reference S_1 centred on and comoving with the generic convective element (non-inertial system). In S_1, the element is at rest with respect to the surrounding medium while it expands / contracts into it. The two reference frames are schematically shown in Fig. B1 (see aslo Pasetto et al. 2014). In this case the motion of a generic element can be described by the integral of the Navier–Stokes equations, i.e. the Bernoulli equation, in which neglecting magnetic fields and viscous terms (typical of high-Reynold-Number fluids in which viscous terms are small compared to inertia terms), the velocity potential approximation can be adopted. In the following, we provide a summary of the SFC theory by Pasetto et al. (2014)
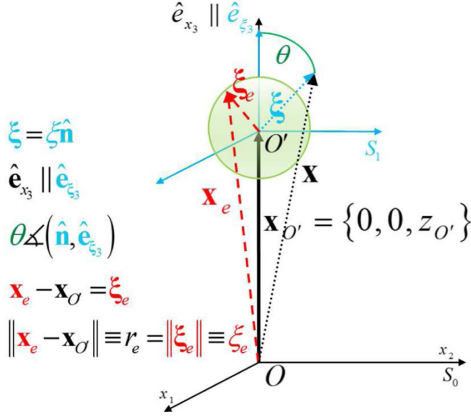
Figure B1. Schematic representation of a convective element seen in the inertial frame S_O and in the comoving frame S_1. The element is represented as spherical body for simplicity. The centre of the sphere indicated as O' corresponds also to the position of the element in S_0. The generic dimension of the convective element as seen in S_1 is indicated by ξ_e.

highlighting the main hypotheses, fundamental equations and the key results.

B2.1 Formulation of the problem and basic equation

As already said, the stellar medium is considered as a perfect fluid with a suitable EoS function of time t and position x as viewed in the inertial system S_0 of Fig. B1. A perfect fluid is intrinsically unstable and turbulent, therefore the higher the Reynolds number the better the above approximation. Furthermore, on macroscopic scales the stellar interiors are represented by a perfect fluid in mechanical and thermodynamical equilibrium and where detailed balance is acquired; all other contributions (viscous $\sim \eta \nabla_x^2 v_0$, centrifugal in presence of rotation $\sim v_0 \times \mathbf{\Omega}$, stratification, induction equation for the presence of magnetic fields, etc,...) except gravity and pressure gradient are neglected; on large integral scales, ℓ, the fluid is irrotational $\omega = \nabla_x \times v_0 = 0$ (i.e. with null vorticity ω) and incompressible (i.e. solenoidal $\frac{\partial \rho}{\partial t} = 0 \Rightarrow \langle \nabla_x, v_0 \rangle = 0$ where, according to the notation adopted after equation (A3), the inner product $\langle \bullet, \bullet \rangle$ here reduces to the ordinary scalar product).[6] Finally, the concept of potential flow can be exploited: the velocity field can be derived from the gradient of suitable potential $v_0 = \nabla_x \Phi_{v_0}$ (see Landau & Lifshitz 1959, chapter 1). This approximation has direct consequences on the applicability of the SFC theory outside astrophysics (whose investigations goes beyond this work). Well know limitations related to the fluid boundaries because of boundary layers (flow in a pipes, aerodynamics, etc.) are of minor interest to the

---

[6] The concept of a large distance scale for incompressibility and irrotationality is defined here from a heuristic point of view: this length scale should be large enough to contain a significant number of convective elements so that a statistical formulation is possible when describing the mean convective flux of energy (see below), but small enough so that the distance travelled by the convective element is short compared to the typical distance over which is possible when describing the mean convective flux of energy (see below), but small enough so that the distance travelled by the convective element is short compared to the typical distance over which significant gradients in temperature, density, pressure etc. can develop (i.e. those gradients are locally small).

astrophysical case if we consider the larger dimensions involved in stars and the consequent very high Reynolds numbers. In S_1, combining the Euler's and mass conservation equation, we can obtain the Bernoulli equation for non-inertial reference frames as Pasetto et al. (2012):

$$\frac{\partial \Phi_{v_0}}{\partial t} + \frac{P}{\rho} + \frac{|v_0|^2}{2} + \Phi_g = f(t) - \langle A, \xi \rangle \tag{B7}$$

where Φ_{v_0} is the velocity potential generating the fluid velocity v_0 and Φ_g the gravitational potential. This relation describes the stellar plasma in which convection is at work.

The main target of any theory of stellar convection is to find solutions of equation (B7) linking the physical quantities characterizing the stellar interiors such as pressure, density, temperature, velocities etc. and the mechanics governing the motion of the convective elements as functions of the fundamental temperature gradients with respect to pressure introduced above, i.e. the radiative gradient ∇_{rad}, the adiabatic gradient ∇_{ad}, the local gradient of the star ∇, the convective element gradient ∇_e and the molecular weight gradient ∇_μ. The problem can be tackled making use of the velocity potential.

B2.2 Velocity potential in an accelerated frame S_1

Let us now introduce the reference frame $S_1 : (O', \mathbf{\xi})$ comoving with and centred on the centre of the generic element. From the geometry shown in Fig. B1, the radius of a generic convective element of spherical shape is indicated as $|x_e - x_{O'}| = r_e$ in S_0 and $|x_e - x_{O'}| = \xi_e$ in S_1. Pasetto et al. (2014) have demonstrated that the total potential flow outside the surface of the moving and expanding/contracting elements in S_1 is given by

$$\Phi' = -\langle v, \mathbf{\xi} \rangle \left(1 + \frac{1}{2} \frac{\xi_e^3}{|\mathbf{\xi}|^3} \right) - \frac{\dot{\xi}_e \xi_e^2}{|\mathbf{\xi}|}, \tag{B8}$$

so that the corresponding velocity in S_1 can be written as

$$v'_0 = \frac{3}{2} \left(\langle v, \hat{n} \rangle \hat{n} - v \right) + \dot{\xi}_e \hat{n} \Big|_{|\xi| = \xi_e}, \tag{B9}$$

with meaning the symbols as in Fig. B1. The above expression is evaluated at the surface of the convective element. It is also easy to show that this equation yields correct results at the surface of the element once written in spherical coordinates with θ the angle between the unitary vectors $\hat{e}_z$ and $\hat{\xi}$. The time derivative of equation (B7) is

$$\frac{\partial \Phi'}{\partial t} \Big|_{|\xi| = \xi_e} = -\frac{3}{2} \xi_e \langle A, \hat{n} \rangle - \frac{3}{2} \dot{\xi}_e \langle v, \hat{n} \rangle - \ddot{\xi}_e \xi_e - 2\dot{\xi}_e^2 \tag{B10}$$

where the relative acceleration of the two reference frames is indicated with A. The inclusion of equation (B8), (B9) and (B10) in equation (B7) leads to the general relation

$$\frac{v^2}{2} \left(\frac{9}{4} \sin^2\theta - 1 \right) - v\dot{\xi}_e \frac{3}{2} \cos\theta + \left(\frac{P}{\rho} + \Phi_g \right) =$$
$$+ A\xi_e \left(\frac{3}{2} \cos\theta - \cos\phi \right) + \ddot{\xi}_e \xi_e + \frac{3}{2} \dot{\xi}_e^2, \tag{B11}$$

where $A = |A|$ is the norm of the acceleration, ϕ the angle between the direction of motion of the fluid as seen from S_1 and the acceleration direction, and θ the angle between the radius ξ in S_1 and the

velocity $\boldsymbol{v}$. It is interesting to note that if we consider approximatively equal the pressure above and below the convective element, we can use the previous equation to obtain an relation for the motion of the barycentre of a non-expanding convective element. At an arbitrary point of this rigid-body approximation we get:

$$\frac{v^2}{2}\left(\frac{9}{4}\sin^2\theta - 1\right) = \frac{A\xi_e}{2}\cos\phi$$

$$-\frac{v^2}{2} = \pm\frac{A\xi_e}{2}$$

$$v^2 = \mp A\xi_e, \tag{B12}$$

which is one of the equations that we want to integrate. A different derivation of this equation will be given in Section B2.4 below. Equation (B11) is the version in spherical-coordinates of a general theorem (see Pasetto et al. 2014, section 4.1) whose applicability is large but of little practical usefulness because of its complexity. Nevertheless, it is the cornerstone of the new theory.

B2.3 The motion-expansion/contraction rate relationship

In order to obtain equations that are analytically treatable, Pasetto et al. (2014) limited their analysis to the linear regime. To this aim they needed a parameter the value of which remains small enough to secure the linearization of the basic equations. If we limit ourselves to *subsonic stellar convection*, it is assumed that the upward/downward velocity of a convective element, $\boldsymbol{v}$, will be much smaller that its expansion rate $\left|\frac{d\xi_e}{dt}\right| \equiv \left|\dot{\boldsymbol{\xi}}_e\right|$, i.e.

$$|\boldsymbol{v}| \ll \left|\dot{\boldsymbol{\xi}}_\mathbf{e}\right|. \tag{B13}$$

This seems to be a reasonable assumption for the majority of the situations we are examining because asymptotically in time the expansion rate of the convective element will tend to the local sound velocity. This allows us to develop a linear theory based on the small parameter $\varepsilon \equiv \frac{|\boldsymbol{v}|}{|\dot{\xi}_\mathbf{e}|} \ll 1$. In this limit case, equation (B11) becomes

$$\ddot{\xi}_e\xi_e + \frac{3}{2}\dot{\xi}_e^2 + \frac{A\xi_e}{2} = 0, \tag{B14}$$

which rules the temporal evolution of the expansion rate of a convective element. The solution of this equation is difficult but feasible and we refer to the appendix of Pasetto et al. (2014) for all mathematical details. The asymptotic solution for $\tau = \frac{t}{t_0} \to \infty$ is of interest here and it is given as a function of the dimensionless size of a generic convective element, $\chi \equiv \frac{\xi}{\xi_0}$, by

$$\chi(\tau) = \frac{1}{4}\tau^2 + \frac{\sqrt{\pi}\,\Gamma\left(\frac{7}{8}\right)}{\Gamma\left(\frac{3}{8}\right)}\tau + \frac{\pi\,\Gamma\left(\frac{7}{8}\right)^2}{\Gamma\left(\frac{3}{8}\right)^2}, \tag{B15}$$

i.e. the asymptotic dependence is $\sim\tau^2$ plus lower order correction terms.[7] As a consequence of this also the time averaged value, that we again define with abuse of notation as $\chi(\tau) = \frac{1}{\tau}\int_0^\tau \chi(\tau')\,d\tau'$,

will grow with the same temporal proportionality:

$$\chi(t) = \frac{1}{\tau}\int_0^\tau \frac{\left(\tau\Gamma\left(\frac{3}{8}\right) + 2\sqrt{\pi}\,\Gamma\left(\frac{7}{8}\right)\right)^2}{4\Gamma\left(\frac{3}{8}\right)^2}\,d\tau$$

$$= \frac{\tau^2}{12} + \frac{\sqrt{\pi}\,\tau\,\Gamma\left(\frac{7}{8}\right)}{2\Gamma\left(\frac{3}{8}\right)} + \frac{\pi\,\Gamma\left(\frac{7}{8}\right)^2}{\Gamma\left(\frac{3}{8}\right)^2} \tag{B16}$$

This is the equation we are going to use below.

B2.4 The acceleration of convective elements

In S_0 the motion of an element of mass m_e is driven by $\boldsymbol{F}_{tot} = \boldsymbol{F}_g + \boldsymbol{F}_P = m_e\ddot{\boldsymbol{x}}$ where $\boldsymbol{F}_g$ is the gravitational force and $\boldsymbol{F}_P$ the force due to the pressure exerted by the surrounding medium, and the total force $\boldsymbol{F}_T$ is acting on the barycenter. In S_1 summing up all the contributions to the pressure on the element surface exerted by the medium from all directions (represented by the normal $\hat{\boldsymbol{n}}$ and the solid angle $d\Omega$) we obtain

$$-\int P\hat{\boldsymbol{n}}d\Omega = \boldsymbol{F}_P = -\left(\frac{2}{3}\pi A\rho\xi_e^3 + \frac{4}{3}\pi g\rho\xi_e^3 + 2\pi\rho v\dot{\xi}_e\xi_e^2\right), \tag{B17}$$

The RHS of this equation contains three terms: the buoyancy force on the convective element $\frac{4}{3}\pi\xi_e^3\rho\boldsymbol{g}$, the inertial term of the fluid displaced by the movement of the convective cell, i.e. the reaction mass $\frac{1}{2}\frac{4}{3}\pi\xi_e^3\rho \equiv \frac{M}{2}$, and a new extra term $-2\pi\xi_e^2\rho v\dot{\xi}_e$ arising from the changing size of the convective element: the larger the convective element, the stronger the buoyancy effect and the larger is the velocity acquired by the convective element. These terms must be included in the Newtonian EoM that reads[8]

$$A_z = -g\frac{m_e - M}{m_e + \frac{M}{2}} - \frac{2\pi\rho}{m_e + \frac{M}{2}}v\dot{\xi}_e\xi_e^2. \tag{B18}$$

The last step now is to work out the vertical component of the acceleration A_z as a function of the temperature gradient ∇, $\nabla_\mu \equiv \frac{\partial\ln T}{\partial\ln\mu}$ (gradient in molecular weight), and ∇_e (convective element). Using the above expression for A_z and applying a lengthy and tedious procedure that takes into account how the densities of the medium and convective element vary with the position, one arrives at the result

$$A_z \simeq g\frac{\nabla_e - \nabla + \frac{\varphi}{\delta}\nabla_\mu}{\frac{3h_p}{2\delta\Delta z} + \left(\nabla_e + 2\nabla - \frac{\varphi}{2\delta}\nabla_\mu\right)}, \tag{B19}$$

with α and δ introduced in Section A3 and $\varphi \equiv \frac{\partial\ln\rho}{\partial\ln\mu}$. Particularly interesting is the case of a homogeneous medium in which $\nabla_\mu = 0$, If we reduced equation to the leading order in $\frac{h_p}{\Delta r} \to \infty$, in a chemically homogeneous convective layer we recover the well know result:

$$A_z \simeq -g\frac{2}{3}\frac{\delta}{h_p}(\nabla_e - \nabla)\Delta r \tag{B20}$$

as asymptotic approximation of order $O\left(\frac{A}{g}\right)$. We note that using equation (B20) we can integrate the EoM of the convective element in S_0: $A_z = \ddot{z} = -g\frac{2}{3}\frac{\delta}{h_p}(\nabla_e - \nabla)z$. Hence, it is easy to verify that a double integration would lead $z = \frac{1}{2}A_0e^{-Xt}\left(e^{2Xt} + 1\right)$

---

[7] The same expression given in Pasetto et al. (2014), their equation (23) or (A6), contained a typos that is amended here. In the RHS of their equation (A6) the factor 2 should read 1/2. Their fig. (A1) is nevertheless unchanged because already plotting the correct (A6) without errors.

[8] In Pasetto et al. (2014), the expression for the same acceleration, their equation (26), contained a typing mistake amended here.

with $X^2 \equiv g \frac{2}{3} \frac{\delta}{h_p} (\nabla - \nabla_e)$ so that the velocity of the convective element will be given by $v = \dot{z} = X v_0 e^{Xt} - \frac{1}{2} X z_0 e^{-Xt} \left(e^{2Xt} + 1 \right) \simeq X^2 t z_0 + O(t)^2$. From this relation we also get $v^2 = A_{\dot{z}}^2 t^2$. But to the leading term $\frac{\xi_e}{\xi_{e0}} \propto \frac{1}{4} \frac{t^2}{t_0^2}$ (see also Section B2.3) so that $t^2 = A_z \frac{t_0^2}{\xi_{e0}}$ and now remembering that $t^2 = -\frac{4}{A_z} \xi_e$, we obtain again the proportionality $v^2 \propto A \xi_e$ already presented in Section B2.2.

It is then immediately evident how this expression implies the Schwarzschild criterion for convective instability ($\nabla_e - \nabla < 0$) as the denominator of equation (B20) is always positive by definition. This is a very important result because it allows us to recover the Schwarzschild and/or Ledoux criteria for instability: even with the new criterion, the convective zones occur exactly in the same regions predicted by the Schwarzschild criterion. For more details on this issue see Pasetto et al. (2014).

B2.5 The final set of equation for the SFC theory

The final step to undertake is to set up the equations for the convective flux, the typical dimension of the convective elements, their velocity etc. The only minor point to comment briefly concerns the possible inclusion of the conductive flux. Since from a formal point of view the conductive flux is customarily expressed in the same way as the radiative one provided the pure radiative opacity is suitably replaced by $\frac{1}{\kappa} = \frac{1}{\kappa_{rad}} + \frac{1}{\kappa_{cnd}}$ with obvious meaning of the symbols (see for instance Cox & Giuli 1968; Kippenhahn & Weigert 1994, or any other textbook), in the equation below we have indicated the portion of total flux carried by radiation plus conduction with the notation $\varphi_{rad/cond}$ and suitably redefined the opacity κ. If conduction is not important all this reduces to the standard radiative flux. The definition of the convective flux is the standard one.

The system of equations derived by Pasetto et al. (2014) that must be solved to determine the convective/radiative-conductive transfer of energy in the atmosphere is

$$
\begin{cases}
\varphi_{rad/cnd} = \frac{4ac}{3} \frac{T^4}{\kappa h_p \rho} \nabla \\[2mm]
\varphi_{rad/cnd} + \varphi_{cnv} = \frac{4ac}{3} \frac{T^4}{\kappa h_p \rho} \nabla_{rad} \\[2mm]
\frac{v^2}{\xi_e} = \frac{\nabla - \nabla_e - \frac{\varphi}{\delta} \nabla_\mu}{\frac{3h_p}{2\delta v t_0 \tau} + \left(\nabla_e + 2\nabla - \frac{\varphi}{2\delta} \nabla_\mu \right)} g \\[2mm]
\varphi_{cnv} = \frac{1}{2} \rho c_p T (\nabla - \nabla_e) \frac{v^2 t_0 \tau}{h_p} \\[2mm]
\frac{\nabla_e - \nabla_{ad}}{\nabla - \nabla_e} = \frac{4ac T^3}{\kappa \rho^2 c_p} \frac{t_0 \tau}{\xi_e^2} \\[2mm]
\xi_e = \left(\frac{t_0}{2} \right)^2 \frac{\nabla - \nabla_e - \frac{\varphi}{\delta} \nabla_\mu}{\frac{3h_p}{2\delta v t_0 \tau} + \left(\nabla_e + 2\nabla - \frac{\varphi}{2\delta} \nabla_\mu \right)} g \chi (\tau).
\end{cases}
\tag{B21}
$$

At each layer, this system is defined once the quantities $\{ T, \kappa, \rho, \nabla_{rad}, \nabla_{ad}, \nabla_\mu, g, c_p \}$ (considered as averages over an infinitesimal region dr *and* time dt) are given as input. This means that the time-scale over which these quantities vary is supposed to be much longer than the time over which the time integration of system is performed.

This paper has been typeset from a TeX/LaTeX file prepared by the author.